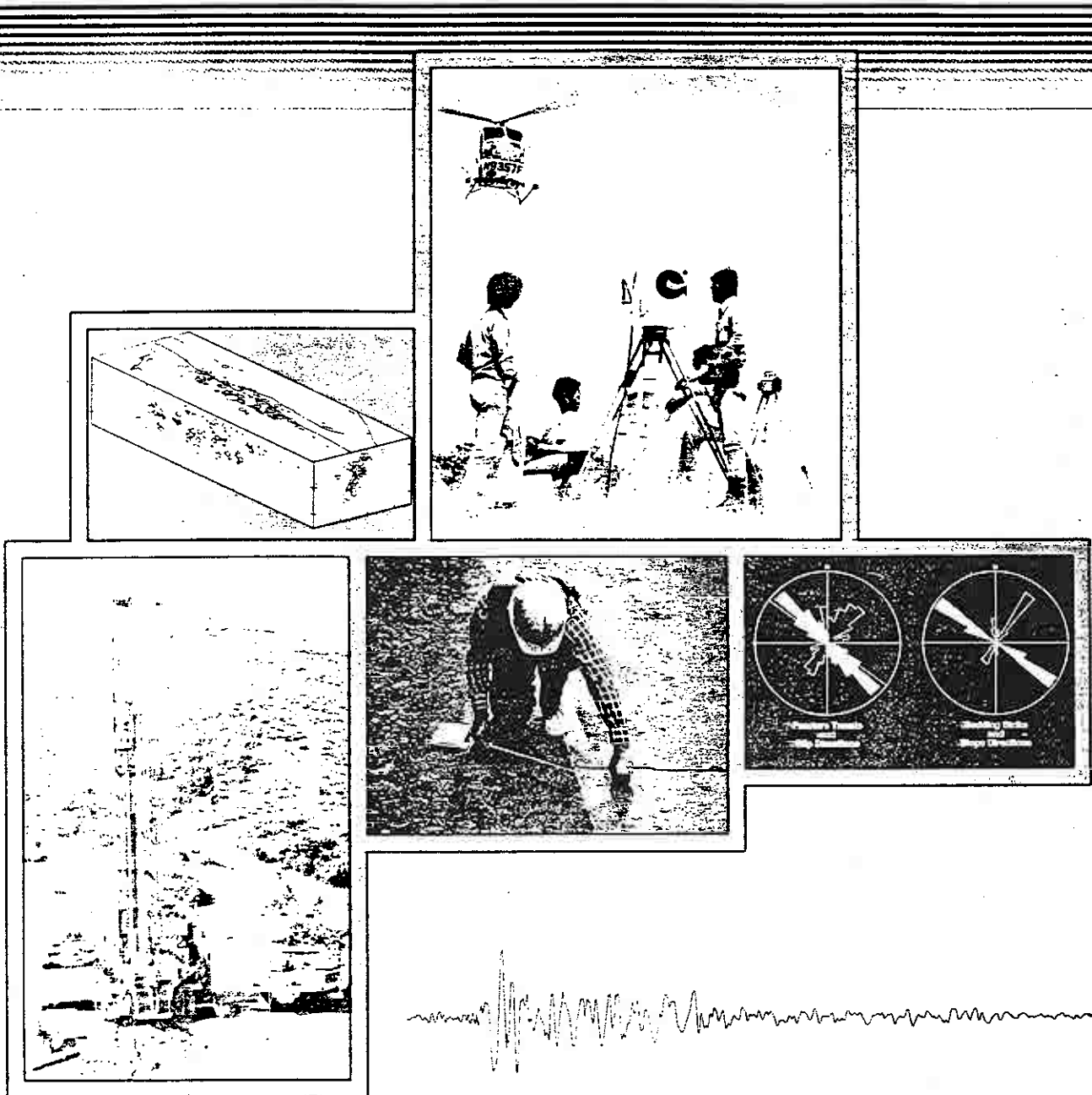# The Loma Prieta, California, Earthquake of October 17, 1989— Preseismic Observations
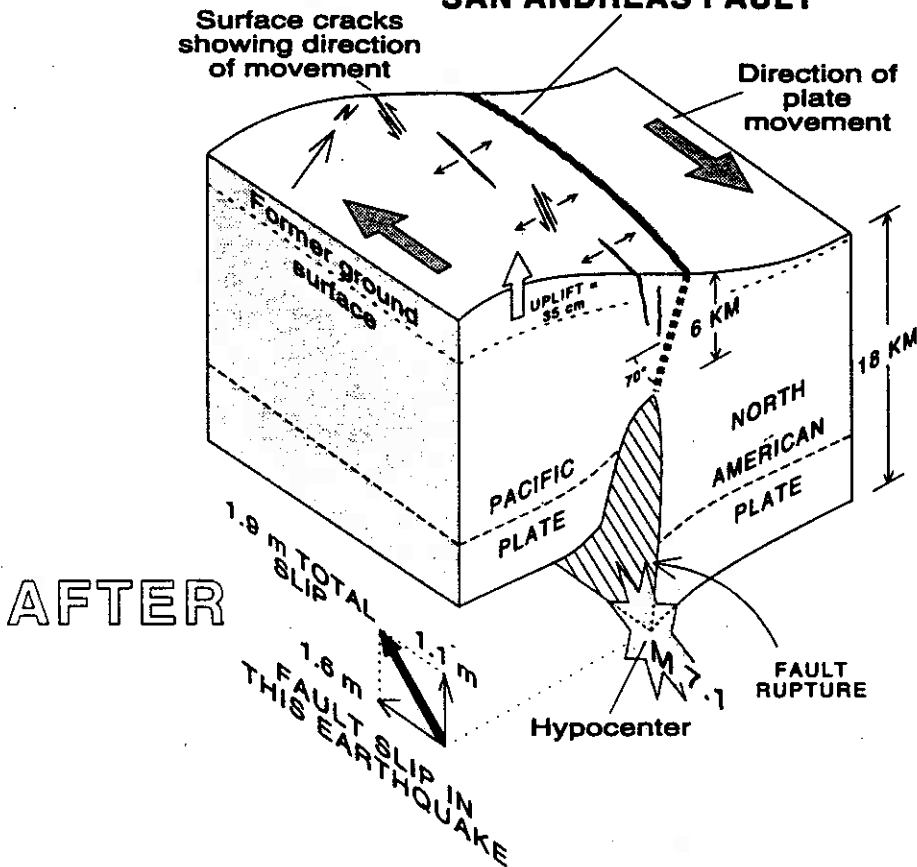
SAN ANDREAS FAULT

BEFORE

EDM
MAGNETOMETER
SEISMOMETER
WATER WELL
STRAINMETER

N

PACIFIC PLATE

NORTH AMERICAN PLATE

SAN ANDREAS FAULT

Surface cracks showing direction of movement

Direction of plate movement

AFTER

Former ground surface

N

UPLIFT = 35 cm

6 KM

70°

18 KM

PACIFIC PLATE

NORTH AMERICAN PLATE

1.9 m TOTAL SLIP

1.6 m FAULT SLIP IN THIS EARTHQUAKE

1.1 m

M

Hypocenter

FAULT RUPTURE
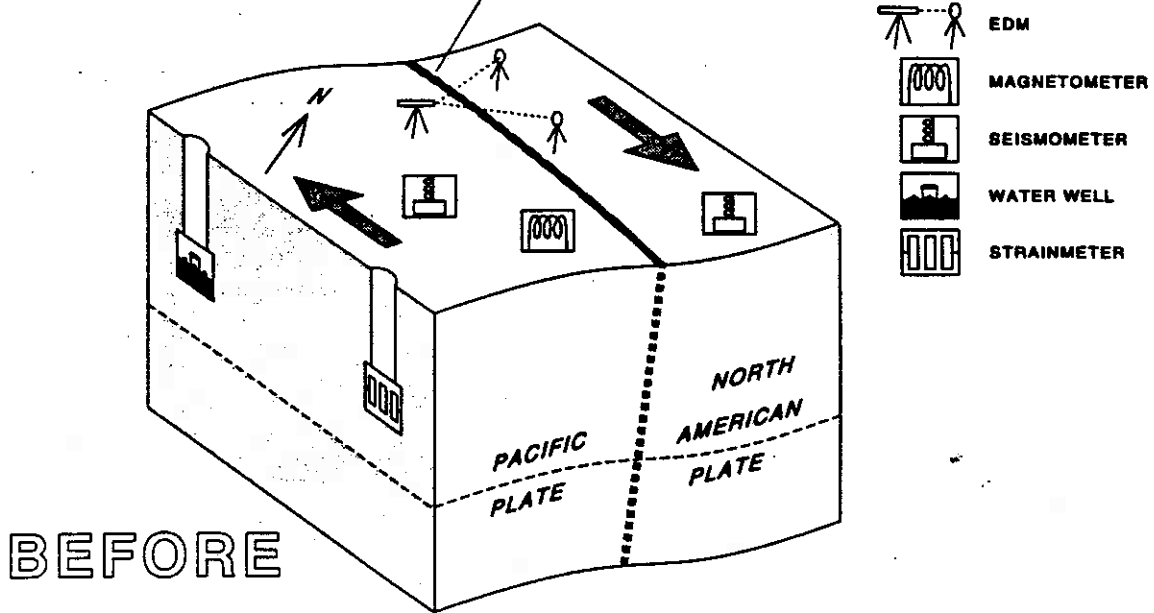
TOP—Distortion in the Pacific and North American plates centered about the San Andreas fault due to the relentless plate movement, showing instruments used to monitor this distortion and the earthquakes that result from it.

BOTTOM—Three-dimensional view of changes in elevation and horizontal displacement due to 1.1 m of oblique slip on section of the San Andreas fault that failed during the Loma Prieta earthquake. Although fault slip did not reach the Earth's surface, intense accelerations from the earthquake generated a complex series of surface cracks, fractures, and landslides around the epicentral region.
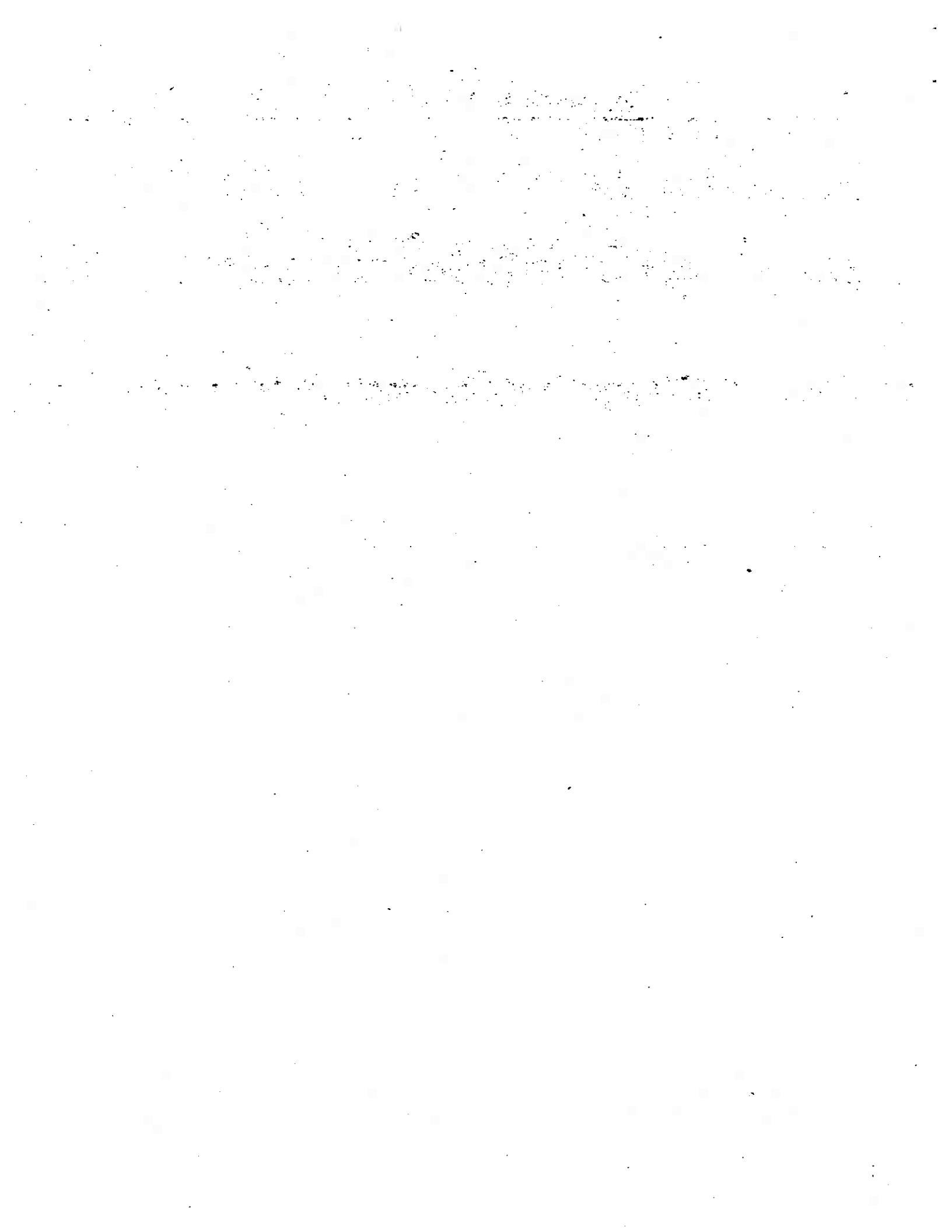
The Loma Prieta, California, Earthquake of October 17, 1989—Preseismic Observations

MALCOLM J.S. JOHNSTON, *Editor*

EARTHQUAKE OCCURRENCE
WILLIAM H. BAKUN and WILLIAM H. PRESCOTT, *Coordinators*

CONTENTS

PRESEISMIC OBSERVATIONS

INTRODUCTION

By Malcolm J.S. Johnston,
U.S. Geological Survey

The October 17, 1989, Loma Prieta, Calif., M_S=7.1 earthquake (see U.S. Geological Survey staff, 1990, for general description) provided the first opportunity in the history of fault monitoring in the United States to gather multidisciplinary preearthquake data in the near field of an M=7 earthquake. The data obtained include observations on seismicity, continuous strain, long-term ground displacement, magnetic field, and hydrology. The papers in this chapter describe these data, their implications for fault-failure mechanisms, the scale of prerupture nucleation, and earthquake prediction in general.

Of the 10 papers presented here, about half identify preearthquake anomalies in the data, but some of these results are equivocal. Seismicity in the Loma Prieta region during the 20 years leading up to the earthquake was unremarkable (see Olson and Hill, this chapter). In retrospect, however, it is apparent that the principal southwest-dipping segment of the subsequent Loma Prieta rupture was virtually aseismic during this period. Two M=5 earthquakes did occur near Lake Elsman near the junction of the Sargent and San Andreas faults within 2.5 and 15 months of, and 10 km to the north of, the Loma Prieta epicenter. Although these earthquakes were not on the subsequent rupture plane of the Loma Prieta earthquake and other M=5 earthquakes occurred in the preceding 25 years, it is now generally accepted that these events were, in some way, foreshocks to the main event.

The most intriguing observations were of increased ultra-low-frequency (ULF) magnetic noise near Corralitos, Calif. (see Fraser-Smith and others, this chapter), during the weeks to months before the earthquake and the months after the earthquake. These observations seem restricted to the frequency band 0.01–10 Hz because lower-frequency noise was not observed at 0.001 Hz at reactivated magnetometer monitoring sites near Corralitos, Calif. (see Mueller and Johnston, this chapter). The observations raise several issues regarding a causative physical mechanism for these signals. Seismic signals also recorded near Corralitos in the frequency band 0.1–10 Hz (see White and Ellsworth, this chapter) show no indication of increased noise, nor do strain signals at more distant sites (see

Johnston and Linde, this chapter). The four most likely physical mechanisms that could generate these signals in the hypocentral region are (1) dynamic changes in electrical conductivity due to strain-driven crack opening and closure; (2) dynamic charge generation due to strain, hydrodynamic, and gas-dynamic processes; (3) electrokinetic effects due to dynamic pore-pressure variations; and (4) piezomagnetic effects resulting from pore-pressure-driven stress changes modifying the magnetic properties of crustal rocks. The absence of detectable seismic or strain signals on nearby seismometers and borehole strainmeters at the 10-μm/s and 10^{-11}/s levels, respectively, strongly limits the size (that is, moment) of the source region driving the above-mentioned mechanisms.

Gladwin and others (this chapter) report possible precursory changes in shear-strain rate in a direction parallel to the San Andreas fault, as determined on a three-component borehole strainmeter some 40 km southeast of the epicenter. Although there initially was some support for these observations in measurements of geodetic lines across the epicentral region (see Lisowski and others, 1990), more careful processing of these data indicates that this support was marginal and that no convincing geodetic anomaly was observed on geodetic lines crossing the epicentral region before the Loma Prieta earthquake (see Lisowski and others, this chapter).

Another intriguing observation is the report of changes in streamflow from streams to the north of the epicenter (see Roeloffs, this chapter). Although this report seems unequivocal, any associated changes in strain appear to have been limited in extent, because no change greater than about 1 microstrain was observed on the borehole strainmeter to the south of the epicentral region during this time (see Johnston and others, this chapter). Observations of changes in geyser activity at Calistoga, Calif., some 177 km from the epicenter (see Silver and others, this chapter), are difficult to explain, particularly when high-quality strain measurements only several tens of kilometers from the epicenter were uneventful and changes in material properties, as indicated by the response to earth tides, were absent (see Linde and others, this chapter).

REFERENCES CITED

Lisowski, Michael, Prescott, W.H., Savage, J.C., and Svarc, J.L., 1990, A possible geodetic anomaly observed prior to the Loma Prieta, California, earthquake: Geophysical Research Letters, v. 17, no. 8, p. 1211–1214.

U.S. Geological Survey staff, 1990, The Loma Prieta, California, earthquake; an anticipated event: Science, v. 247, no. 4940, p. 286–293.

PRESEISMIC OBSERVATIONS

SEISMICITY IN THE SOUTHERN SANTA CRUZ MOUNTAINS DURING THE 20-YEAR PERIOD BEFORE THE EARTHQUAKE

By Jean A. Olson and David P. Hill,
U.S. Geological Survey

CONTENTS

ABSTRACT

We examine the spatial distribution of well-located earthquakes in the 20-year period before the earthquake, and their association with faults, along a 100-km-long extent of the southern Santa Cruz Mountains. Several faults in the study area are clearly associated with background seismicity since 1969. Notably, however, the principal southwest-dipping part of the Loma Prieta rupture below 10-km depth was virtually aseismic. Most of the seismicity in the study area was associated with the creeping section of the San Andreas fault south of Pajaro Gap and adjacent faults to the east. However, the area centered 11 km north-northeast of the Loma Prieta main shock, near the intersection of the San Andreas and Sargent fault traces, also produced persistent seismicity, albeit at a much lower rate. This seismicity includes the 1988 (M=5.3) and 1989 (M=5.4) Lake Elsman earthquakes, which have fault-plane solutions consistent with oblique strike-slip and reverse-slip components on a plane that dips about 65° NE. These events stand out against the background seismicity because they are a full unit of magnitude larger than other events within a 15-km radius for at least 74 years and be-

cause they occurred within 16 and 2½ months, respectively, of the Loma Prieta earthquake. In the 25 years before the earthquake, however, two other M=5 events occurred along the Loma Prieta rupture zone: the 1964 (M=5.0) and 1967 (M=5.3) Corralitos earthquakes, located approximately 17 km east and 10 km southeast, respectively, of the Loma Prieta main shock. In view of these other M=5 events along the rupture zone, the temporal proximity of the Lake Elsman earthquakes and the Loma Prieta earthquake may be coincidental and not necessarily precursory. Thus, with the possible exception of the Lake Elsman earthquakes, seismicity patterns in the 20-year period before the Loma Prieta earthquake were essentially stable, showing no clear precursory changes.

INTRODUCTION

The October 17, 1989, Loma Prieta earthquake was the first major (M≥7) earthquake to occur anywhere along the main branch of the San Andreas fault zone since the great (M=8) San Francisco earthquake of 1906. Because the Loma Prieta earthquake occurred within the confines of the U.S. Geological Survey's (USGS) dense, regional seismic network that began operation in the late 1960's (Eaton, 1989), we have an exceptional record of well-located microearthquakes in the preceding 20 years. In this paper, we document the spatiotemporal distribution of microearthquakes from 1969 up to the time of the Loma Prieta earthquake. Two noteworthy aspects of this preearthquake seismicity are that (1) the southwest-dipping part of the Loma Prieta rupture below 10-km depth was virtually quiescent in the 20-year period before the earthquake, and (2) only two earthquakes stand out as unusual in this period: the 1988 (M=5.3) and 1989 (M=5.4) Lake Elsman earthquakes, located 10 and 12 km, respectively, north-northeast of the Loma Prieta main shock. The record of M≥5 earthquakes since 1910, however, includes two other M=5 events: the 1964 (M=5.0) and 1967 (M=5.3) Corralitos

earthquakes, located approximately 17 km east and 10 km southeast, respectively, of the Loma Prieta main shock.

Previous retrospective studies using data from the USGS' Central California Seismic Network (Calnet) to focus on seismicity patterns along the San Andreas fault zone through the the Santa Cruz Mountains before the earthquake include those by King and others (1990), Olson (1990), and Seeber and Armbruster (1990). Ellsworth (1990) and Hill and others (1990, 1991) provided an overview of the seismotectonic fabric and earthquake history of the San Andreas fault system and extensive references to related studies.

SEISMOTECTONIC SETTING

The San Andreas fault system in central California accommodates the relative motion between the Pacific and North American plates by right-lateral, strike-slip displacement distributed along several subparallel branches (fig. 1). The main branch, which cuts through the Santa Cruz Mountains and the San Francisco peninsula with a northwestward strike, juxtaposes Cretaceous granitic basement of the Salinian block on the west against melange of the Mesozoic Franciscan Complex and the Great Valley sequence on the east, with a demonstrated post-Miocene off-
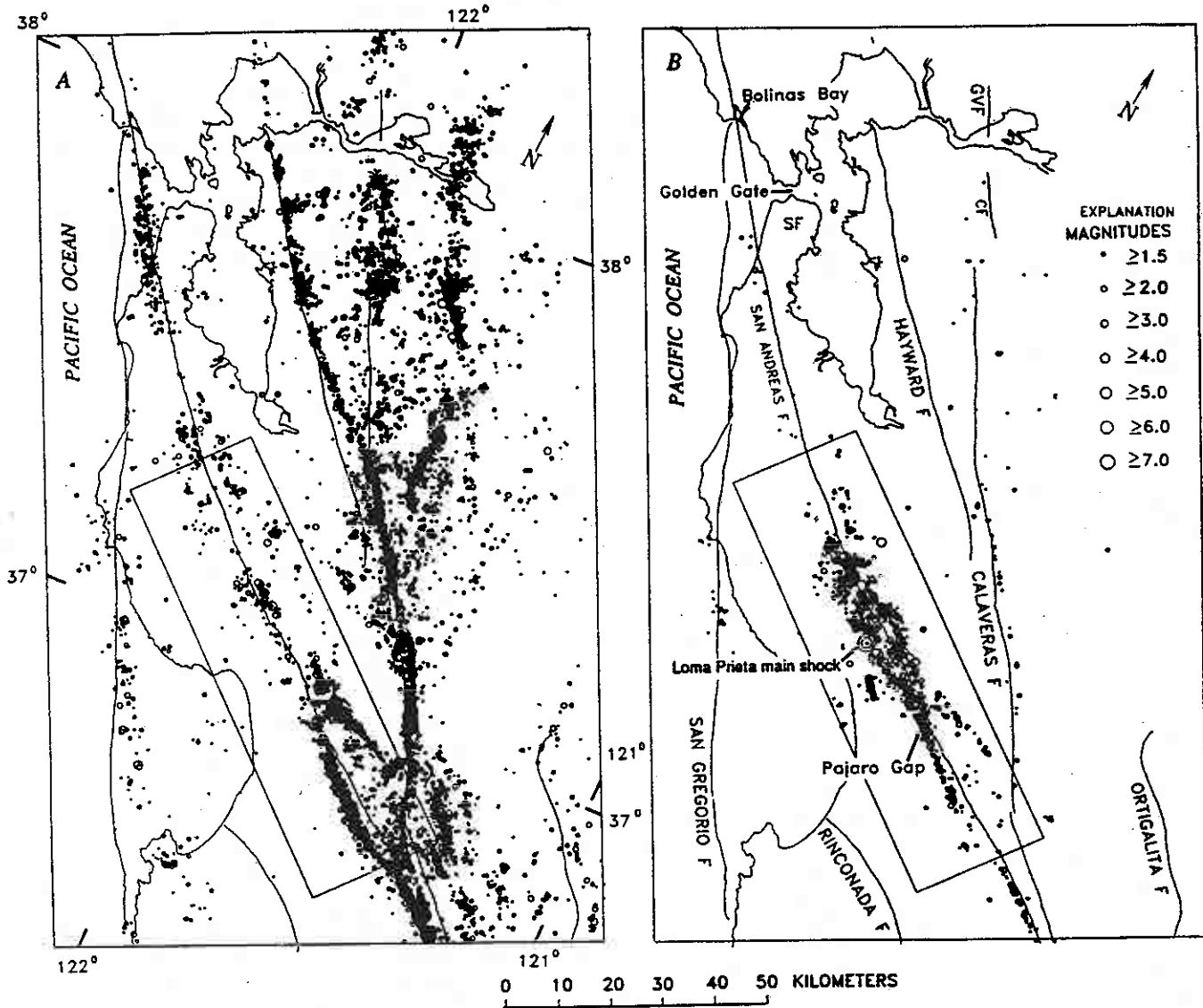

Figure 1.—Santa Cruz Mountains area, Calif., showing locations of epicenters of (A) preearthquake events of M≥1.5 since January 1, 1969 (G.m.t.), and (B) events of M≥1.5 between October 18 and December 31, 1989 (G.m.t.), including Loma Prieta main shock and aftershocks. Rectangle delimits study area. CF, Concord fault; GVF, Green Valley fault; SF, San Francisco.

set of more than 300 km (Irwin, 1990). To the west, the San Gregorio fault skims the coast of the peninsula and merges with the principal branch of the San Andreas fault north of the Golden Gate near Bolinas Bay (fig. 1*B*). To the east, the Calaveras fault splays northward into the Hayward, Calaveras, and Green Valley-Concord faults.

The sections of the San Andreas fault system marked by dense lineations of epicenters in figure 1*A* show evidence of active fault creep. The central, creeping section of the main branch, which extends from the latitude of Pajaro Gap for 200 km to the southeast (see Hill and others, 1991), has a maximum, long-term creep rate of 30 mm/yr in the central part of this section, close to the geodetically derived rate of 33 mm/yr measured across a 60-km-wide zone (Thatcher, 1990). Thus, along the central part of this creeping section, creep accommodates most of the slip, and the crustal blocks on either side of the fault are accumulating little, if any, shear strain (Thatcher, 1990). Active fault creep, however, is partially shunted to the north along the Calaveras-Hayward fault system; and the creep rate along the section of the San Andreas fault south of Pajaro Gap and its junction with the Calaveras fault ranges from 8 to 14 mm/yr (Burford and Harsh, 1980; Schulz and others, 1982). Creep rates along the Calaveras-Hayward branches also diminish northward, from 13 mm/yr along the southern section of the Calaveras fault to 3–6 mm/yr along the northern sections of the Calaveras and Hayward faults, respectively (see Thatcher, 1990).

In contrast, the section of the fault that ruptured in the 1906 earthquake produces only sparsely scattered microearthquake activity and no fault creep. This section of the fault extends for more than 300 km between the north end of the creeping section along the main branch near Pajaro Gap and Cape Mendocino (see Hill and others, 1991). Before the Loma Prieta earthquake, geodetic measurements indicated that this entire section of the fault was locked

since the 1906 earthquake and that shear strain was accumulating in the crustal blocks on either side of the fault (Thatcher, 1990).

The Santa Cruz Mountains section of the San Andreas fault zone that produced the Loma Prieta earthquake is canted nearly 10° counterclockwise to the N. 38° W. strike of the principal branch of the San Andreas fault through most of the central California Coast Ranges (fig. 1). This slight restraining bend in the fault zone acts to increase the local component of crustal convergence across the fault zone, which, at least in part, is responsible for uplift of the Santa Cruz Mountains, together with terrace uplift along the coastline (Anderson, 1990; Valensise and Ward, 1991) and Holocene displacement on the host of reverse faults locally subparallel to the San Andreas fault zone (McLaughlin, 1974). As Dietz and Ellsworth (1990) pointed out, the component of reverse slip associated with the earthquake is kinematically consistent with oblique convergence across this restraining bend.

The earthquake resulted from a 35- to 40-km-long, bilateral rupture beneath the Santa Cruz Mountains, with nearly equal parts of reverse slip and dextral strike-slip displacement along a plane dipping 70° SW. beginning at 18-km depth and extending to within 5 to 10 km of the surface. The 5-km depth to the top of the rupture surface is consistent with a planar, geodetic faulting model (Lisowski and others, 1990), although most seismologic data suggest that the primary, southwest-dipping part of the rupture was below about 10-km depth (Dietz and Ellsworth, 1990; Beroza, 1991; Steidl and others, 1991; Wald and others, 1991). The rupture began 18 km northwest of Pajaro Gap and extended from the main-shock hypocenter about 13 km to the northwest and 20 km to the southeast (Beroza, 1991). The aftershock zone extended about 60 km beyond the rupture itself (Dietz and Ellsworth, 1990). By October 31, 1989, the south end of the aftershock zone overlapped the seismically active central section of the San Andreas fault
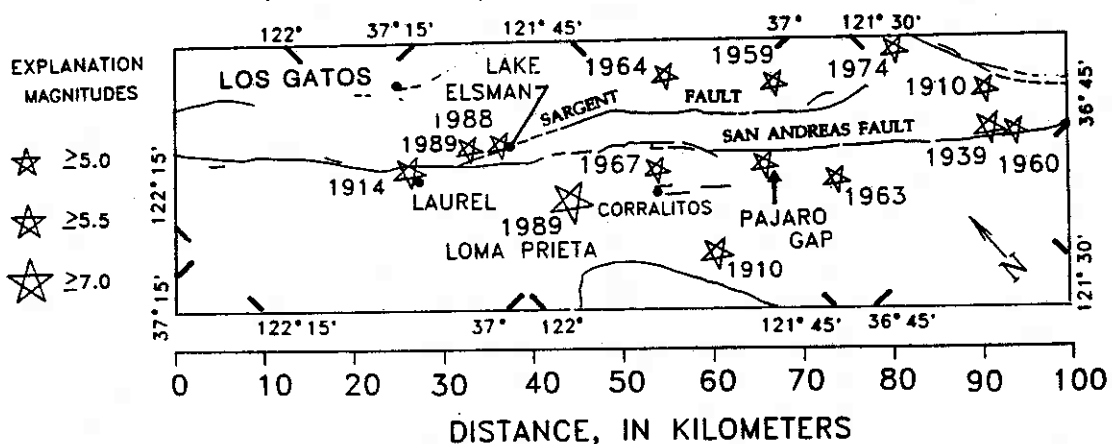
Figure 2.—Study area, showing locations of epicenters of preearthquake events of M≥5 since March 11, 1910 (G.m.t.), and October 18, 1989 (G.m.t.), Loma Prieta main shock. Epicenters of events between 1910 and 1968 from Bolt and Miller (1975) and Toppozada and others (1978); epicenters of events since 1969 from Calnet catalog. Fault lines: solid, well located; dashed, approximately located or inferred; dotted, concealed by younger rocks or by lakes or bays.

by about 3 km (Dietz and Ellsworth, 1990). The Loma Prieta rupture zone falls within the southernmost 40 km of the fault zone that broke in the 1906 earthquake, although geodetic evidence suggests that the Loma Prieta rupture surface is distinct from the 1906 rupture surface, which appears to have involved pure dextral strike-slip displacement above about 10-km depth (Segall and Lisowski, 1990).

The record of instrumentally recorded earthquakes in the San Francisco Bay area is complete for magnitudes of 5 and greater since at least 1910 (Bolt and Miller, 1975; Toppozada and others, 1978). The Seismograph Station of the University of California, Berkeley (UCB), operated 6 stations in north-central California by 1940 and 17 by 1972. Since 1910 and before the earthquake, a total of 13 $M \geq 5$ earthquakes were located in the study area (fig. 2), at least 4 of which occurred along the length of the Loma Prieta rupture zone within a 15-km-wide zone centered on the San Andreas fault trace: the 1964 ($M=5.0$) and 1967 ($M=5.3$) Corralitos earthquakes, and the 1988 ($M=5.3$) and 1989 ($M=5.4$) Lake Elsman earthquakes. Location errors for the Corralitos earthquakes are about 10 km, and for events before the 1960's greater than 10 km. Given the uncertainties in the epicentral locations of these pre-1960 earthquakes, other events, such as the 1910 ($M=5.5$), 1914 ($M=5.5$), 1954 ($M=5.3$), and 1959 ($M=5.3$) earthquakes, may also have occurred along the Loma Prieta rupture zone.

DATA AND LOCATION METHOD

The USGS began installing dense clusters of telemetered seismic stations along the San Andreas fault in central California in 1967. By 1969, Calnet included 250 stations, permitting the uniform detection and location of $M \geq 1.5$ earthquakes occurring throughout central California (Eaton and others, 1970; Lee and Stewart, 1981; Eaton, 1989).

The Calnet-catalog hypocenters in the study area were calculated with the earthquake-location program HYPOIN-VERSE (Klein, 1989). The velocity model used by Calnet to locate events within the study area (fig. 3A) is a one-dimensional model based on the model calculated by Dietz and Ellsworth (1990) to locate Loma Prieta aftershocks (Fred Klein, written commun., 1991). Both models consist of distinct P-wave-velocity profiles and station corrections for stations on either side of the San Andreas fault (fig. 3B). The main difference between the Calnet model and that of Dietz and Ellsworth is that the Calnet model has a linear velocity gradient within each layer and Dietz and Ellsworth's has homogeneous layer velocities. Another slight difference is that more stations outside the southern Santa Cruz Mountains area were used by Calnet to locate earthquakes in that area. The difference between hypocenter locations using each of these models is generally less than 1 km, and differences in the overall distribution of relative locations are neglibible.

The magnitudes of preearthquake events used in this study are duration magnitudes (M_F) (Eaton, 1992) except for a few events with $M_F \geq 4.0$, for which amplitude magnitudes from the UCB catalog (M_a) were substituted. We made this substitution because for events of $M_F < 4.0$, M_F closely approximates M_L, whereas for events of $M_F \geq 4.0$ it does not (J.P. Eaton, oral commun., 1991).

Double-couple fault-plane solutions were calculated in this study by using hand-picked P-wave first-motion observations and the FPFIT algorithm of Reasenberg and Oppenheimer (1985), which uses a grid-search procedure to minimize first-motion discrepancies.

SEISMICITY AND PRINCIPAL FAULTS

Maps, cross sections, and distance-time plots of all the well-located hypocenters in the study area are shown in figures 4 through 7. These plots, which have a common scale and orientation, provide a four-dimensional depiction of the seismicity in the study area for the 20-year period before the earthquake. Distances from northwest to southeast shown in these figures correspond to the parenthetic distances used in the following descriptions of seismicity patterns.

The extent of the aftershock zone with respect to the preearthquake seismicity since 1969 is illustrated in figure 4. To the south, the aftershocks extend 3 km into the dense lineation of epicenters along the creeping section of the San Andreas fault; to the north, they extend 3 to 5 km beyond the persistent seismicity cluster (km 30–40, figs. 4A, 4C) near Lake Elsman where the Sargent fault intersects the San Andreas fault. Preearthquake seismicity along the intervening section of the aftershock zone was characterized by sparse events scattered several kilometers on either side of the San Andreas fault trace. In cross section (fig. 4C), the preearthquake seismicity delineates a broad, U-shaped distribution that forms a lower bound to the alongstrike distribution of aftershocks (fig. 4D). This depth distribution was first noted by Moths and others (1981) and Lindh and others (1982) for seismicity between 1969 and 1981. A comparison of the cross section in figure 4C with the series of maps showing epicenters within successive 5-km depth intervals in figure 5 emphasizes that the U-shaped seismicity distribution is common to several structures as far as 5 km on either side of the San Andreas fault. As illustrated in the series of cross sections in figure 6, this U-shaped depth distribution has been persistent since at least 1969. Within the section of the fault zone north of Pajaro Gap (km 67, fig. 4), preearthquake seismicity (figs. 4A, 4C) and aftershocks (figs. 4B, 4D) generally do not coincide, whereas south of Pajaro Gap, there is some overlap with preearthquake hypocenters.

Figure 7 indicates that the epicentral patterns were essentially stable in the 20-year period before the earth-
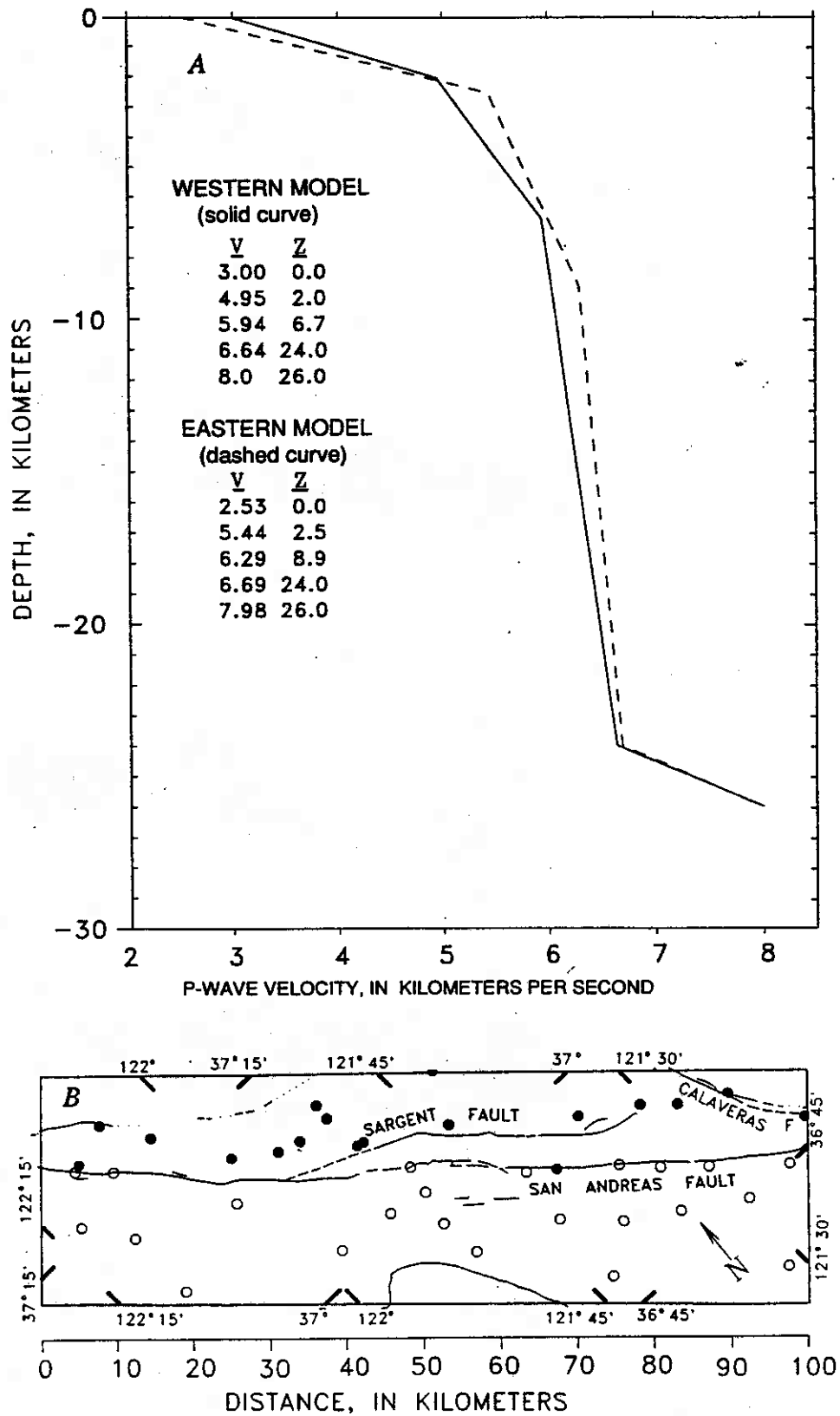
Figure 3.—Velocity model. *A*, Focal depth (*Z*) versus *P*-wave velocity (*V*) of crust beneath the Santa Cruz Mountains on east and west sides of the San Andreas fault trace. *B*, Study area (fig. 1), showing locations of Calnet seismic stations. Dots and circles, stations for which eastern and western models are used, respectively. Fault lines: solid, well located; dashed, approximately located or inferred; dotted, concealed by younger rocks or by lakes or bays.
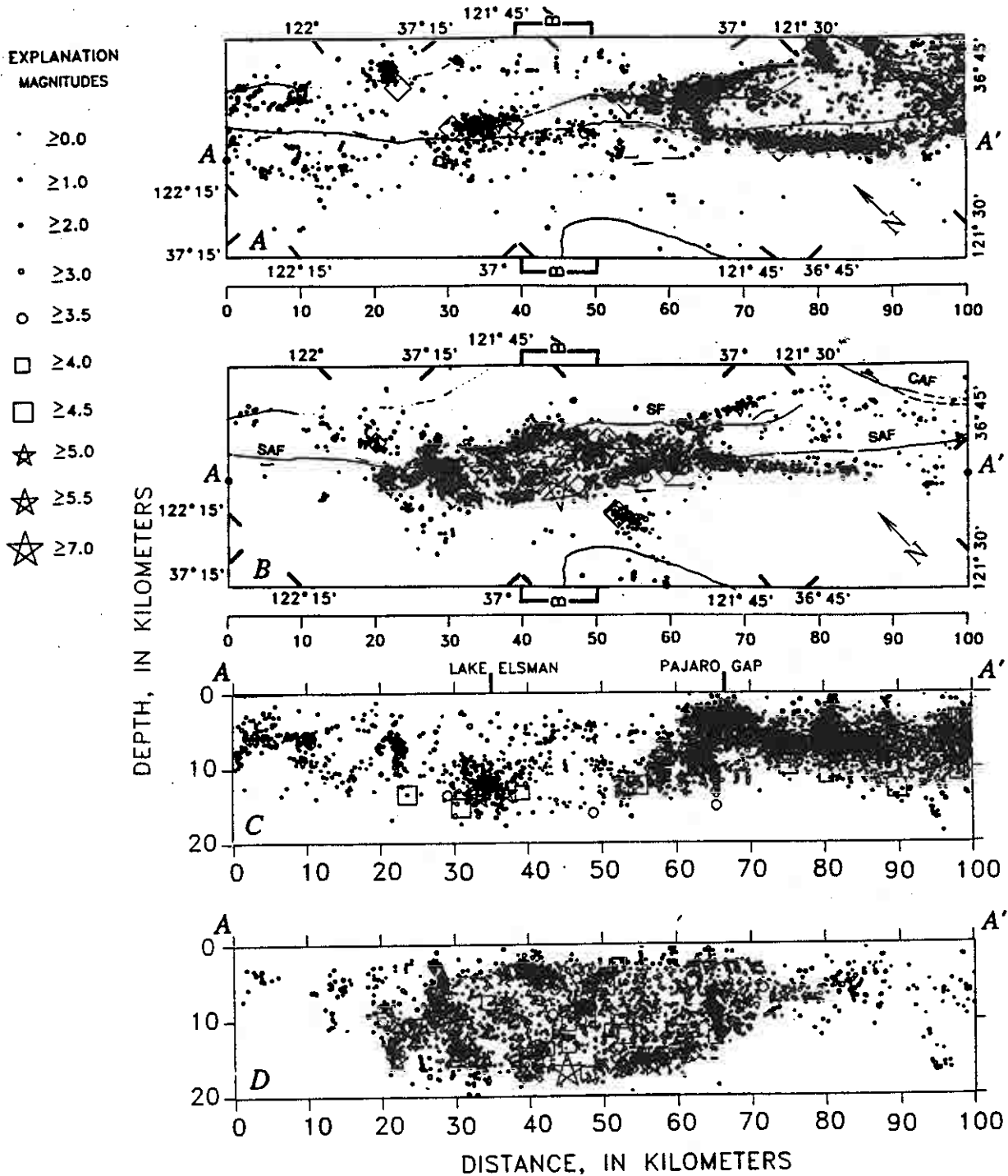
Figure 4.—Maps (A, B) of study area (fig. 1) and cross sections (C, D) along line A–A', showing locations of epicenters and hypocenters of preearthquake events since January 1, 1969 (G.m.t.) (A, C), and of Loma Prieta main shock (star at km 45) and aftershocks between October 18 and December 31, 1989 (G.m.t.) (B, D). Preearthquake subset includes 76 percent of all events located by Calnet in study area, which includes only events located by at least eight stations, with rms traveltime residual of less than 0.2 s, horizontal error of less than 1.0 km, and depth error of less than 2.0 km. Note that events located near five quarry blastsites in depth ranges of respective, known quarry hypocenters are omitted; two of these blastsites were located at surface trace of the San Andreas fault at km 73 and 92, in which case all events of less than 3-km depth, whether actual quarry blasts or earthquakes, are omitted. Zone B–B' shows location of cross sections in figure 8. CAF, Calaveras fault; SAF, San Andreas fault; SF, Sargent fault. Fault lines: solid, well located; dashed, approximately located or inferred; dotted, concealed by younger rocks or by lakes or bays.

Figure 5.—Study area (fig. 1), showing locations of epicenters of preearthquake events shown in figure 4A within depth intervals of (A) 0–5 km, (B) 5–10 km, (C) 10–15 km, and (D) 15–20 km. Fault lines: solid, well located; dashed, approximately located or inferred; dotted, concealed by younger rocks or by lakes or bays.
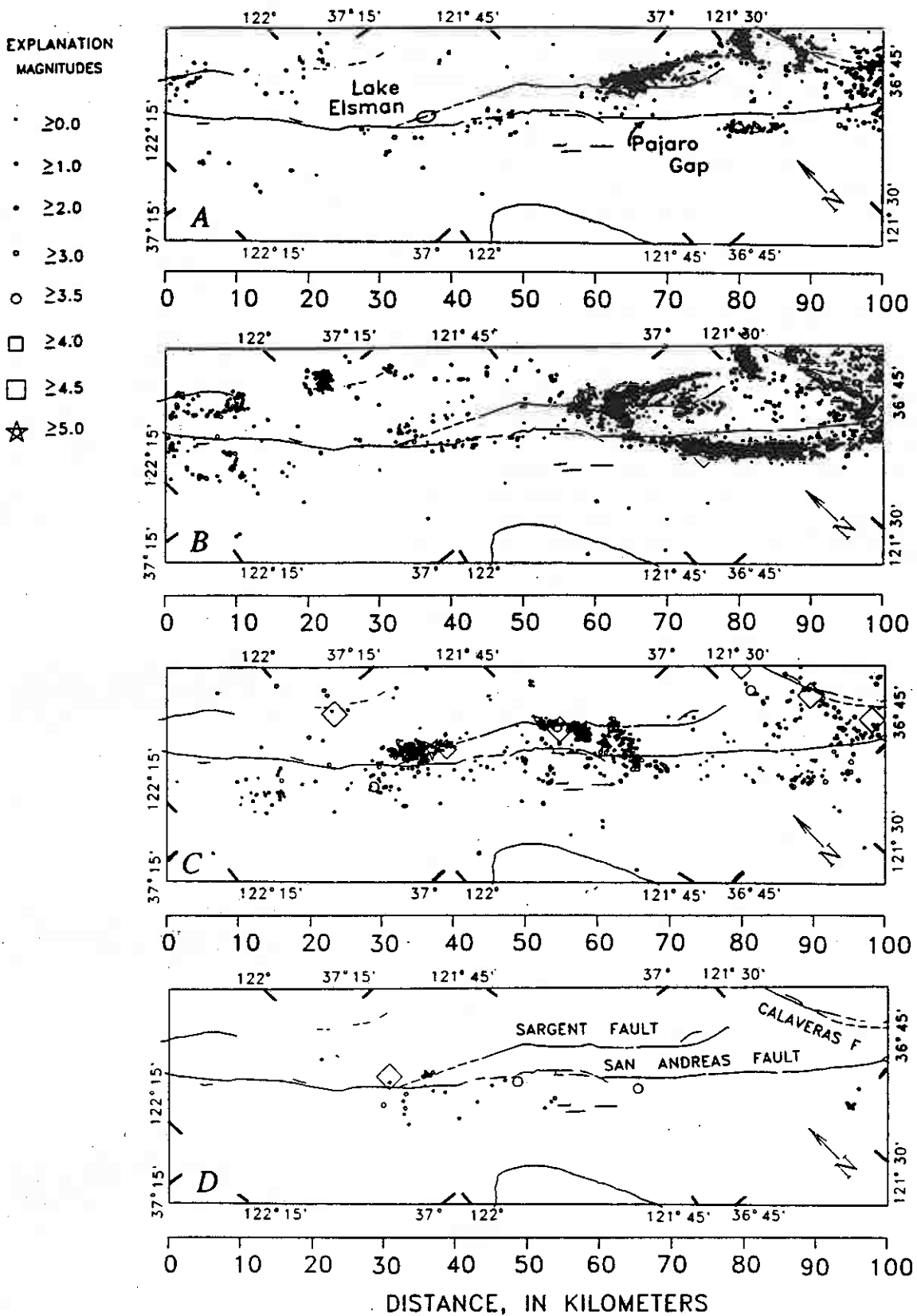
quake. Both the UCB catalog for 1910–72 (Bolt and Miller, 1975) and the historical record of major earthquakes (Ellsworth, 1990) suggest that this basic pattern persisted since the 1906 earthquake, except for such poorly located $M \geq 5$ earthquakes as the 1967 Corralitos (M=5.3) earthquake that may have occurred in an otherwise seismically quiescent area (see figs. 2, 4A).

In the following sections, we elaborate on some of the more noteworthy aspects of these preearthquake seismicity patterns.

AREA SOUTHEAST OF PAJARO GAP

A dense concentration of epicenters is closely aligned with the creeping section of the San Andreas fault south of Pajaro Gap (fig. 4A) at focal depths ranging from 2 to 12 km (figs. 4C, 5). The offset of these epicenters 3 to 5 km southwest of the surface trace of the San Andreas fault reflects systematic hypocentral mislocations associated with a strong contrast in P-wave velocity across the fault, although some of the offset may also reflect a steep (–70°

SW.) dip of this section of the San Andreas fault (Pavoni, 1973; Spieth, 1981).

Dense alignments of epicenters also occur along the south end of the Calaveras fault trace and subparallel to but northeast of the southern section of the Sargent fault trace (km 83–100 and 48–79, respectively, fig. 4A). The southeast termination of the latter alignment occurs at the conjugate, southwest-northeast-oriented Busch Ranch fault (Rogers, 1980). An alignment of epicenters along the Busch Ranch fault (km 78–82, fig. 4A) is primarily associated with the M=5.2 earthquake on Thanksgiving Day (Nov. 28) 1974 and its aftershocks (see figs. 2, 7). A short, transverse alignment of epicenters spans the distance between the San Andreas fault trace (km 63, fig. 4A) and the Sargent fault trace (km 50, fig. 4A). This transverse alignment is not associated with any recognized surface fault. Like the events aligned along the adjacent section of the San Andreas fault, most of the earthquakes northeast of the Sargent fault have focal depths of 2 to 10 km (figs. 4C, 5). The events between the San Andreas and Sargent faults, however, extend slightly deeper, mostly from 6 to 14 km (fig. 5).
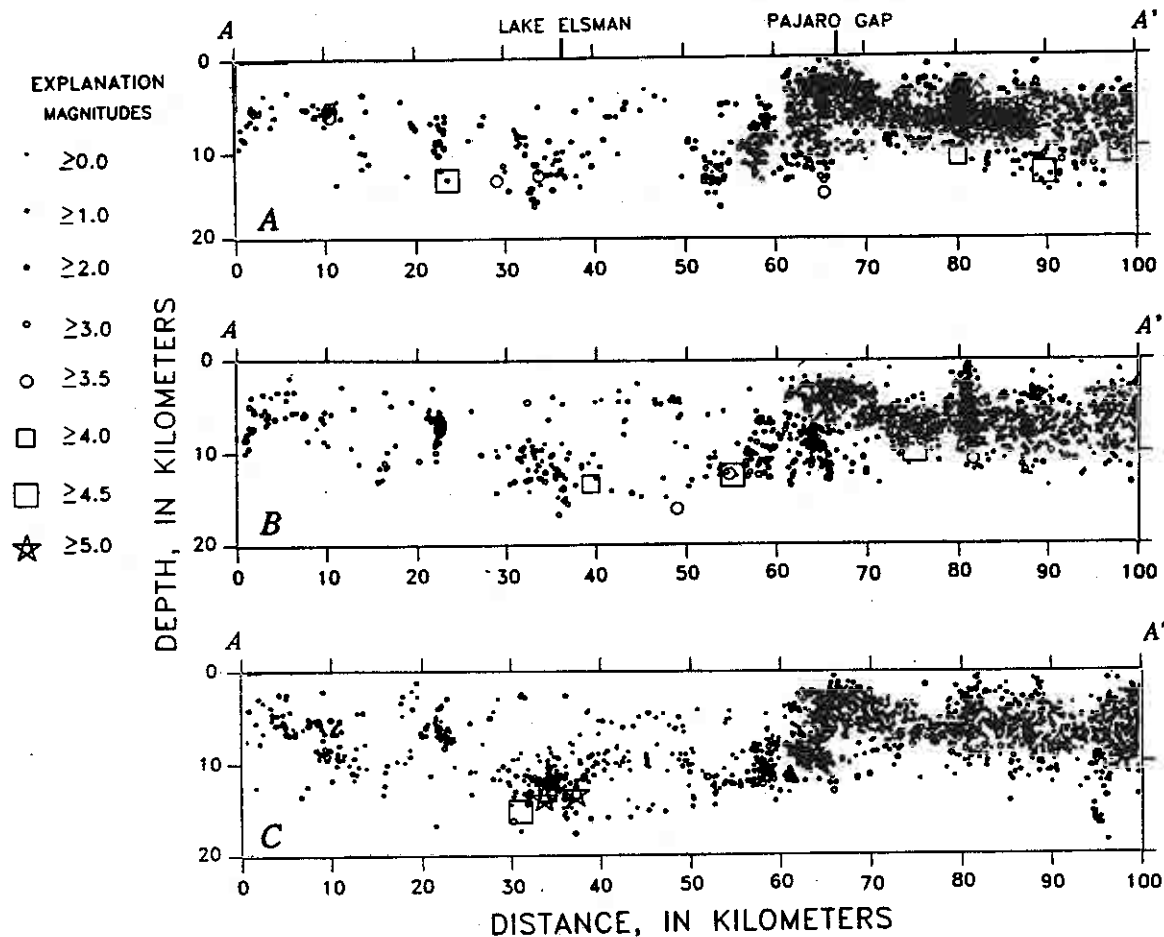

Figure 6.—Cross sections along line A–A' (fig. 4), showing locations of preearthquake events along strike of the San Andreas fault during years (A) 1969–75, (B) 1976–82, and (C) 1983–89 (G.m.t.).

AREA NORTHWEST OF PAJARO GAP

A few preearthquake events (km 26–49, figs. 4A, 4C) have focal depths of as much as 16 km beneath the section of the San Andreas fault trace east of the main-shock hypocenter (km 45, figs. 4B, 4D), but these events are too few to delineate a single planar structure. They could be associated with a continuous, vertical fault beneath the San Andreas fault trace (Olson, 1990) or, alternatively, with discontinuous, subparallel faults, as suggested by Ellsworth and others (1990). A view of these events in a cross section perpendicular to the strike of the San Andreas fault trace (fig. 8A) shows their vertical alignment beneath the fault trace, but the reality of this alignment depends strongly on a single M=3.5 event in 1980 at 16-km depth (km 48, figs. 4A, 4C, 7), which has a fault-plane solution with nearly pure strike slip and a vertical, northwest-striking nodal plane (Olson, 1990). A comparison with Loma Prieta aftershocks (fig. 8B) shows that this event is located about 3.5 km northeast of the principal,
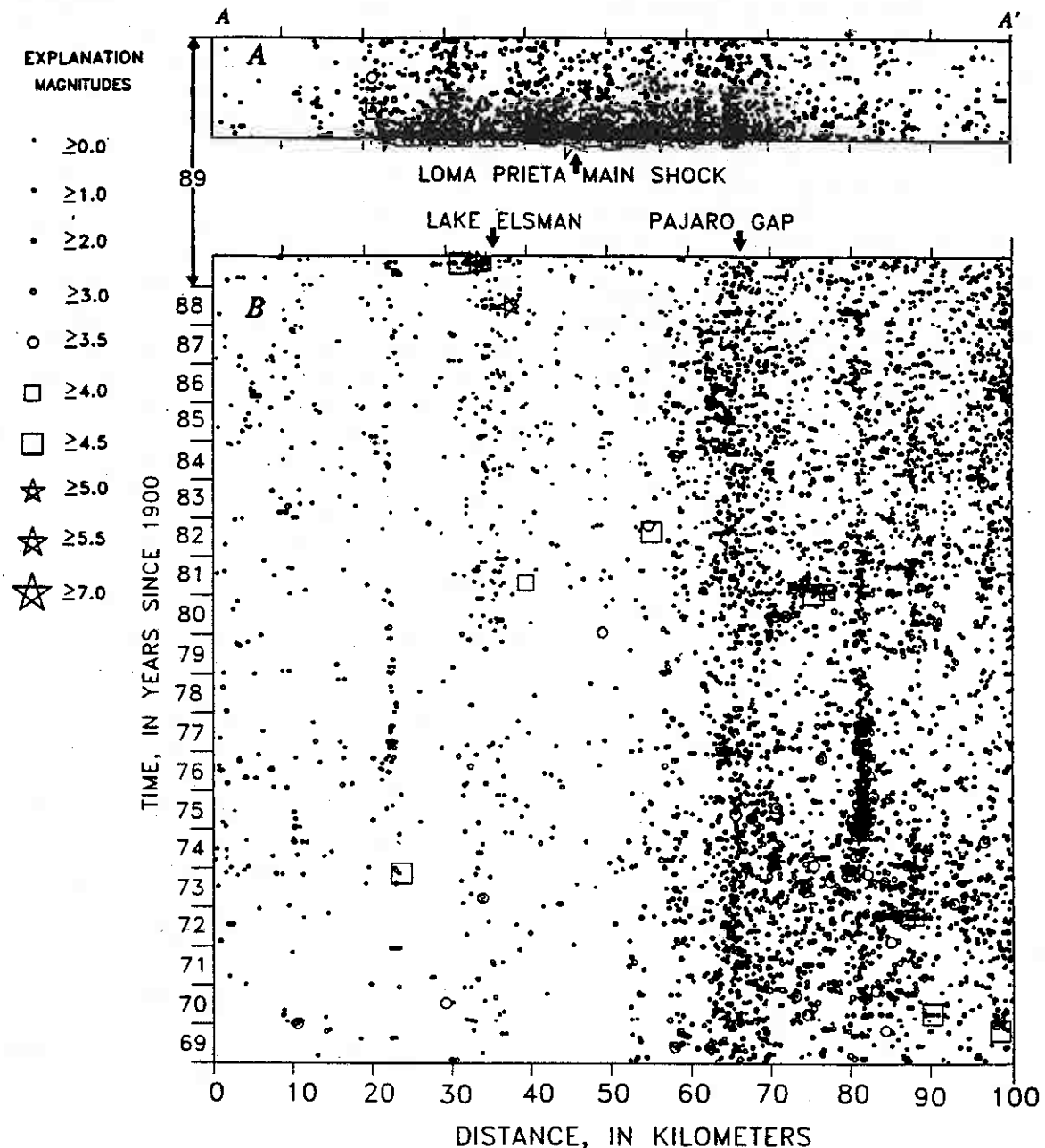

Figure 7.—Time versus distance along line A–A' (fig. 4) for (A) Loma Prieta main shock and aftershocks and (B) preearthquake events. Conspicuous, persistent cluster of events at km 80 is Thanksgiving Day 1974 earthquake (M=5.2) and its aftershocks on the Busch Ranch fault (Rogers, 1980).

southwest-dipping volume of aftershocks. A vertical projection of the San Andreas fault trace would intersect this volume of aftershocks at about 10-km depth. We note that no events occurred within 3.5 km of the main-shock hypocenter in the 20-year period before the earthquake.

A 10-km-long cluster of epicenters (km 30–40, fig. 4A) occurs near the intersection of the Sargent fault trace with the San Andreas fault near Lake Elsman. This cluster includes the June 27, 1988 (M=5.3) and August 8, 1989 (M=5.4) Lake Elsman earthquakes (km 36 and 33, respectively, figs. 2, 6C, 7). Events in this cluster have focal depths concentrated between 11 and 15 km (figs. 4C, 5). All of the events in this cluster since 1969 and before the 1988 Lake Elsman earthquake were of M<3, except for an M=3.5 event in 1973 (km 33, figs. 6A, 7) and an M=4.0 event in 1981 (km 39, figs. 4A, 6B, 7). A notable aspect of the Lake Elsman earthquakes is that only one aftershock of M≥1.5 occurred within 10 days of the 1988 earthquake, whereas nine occurred within 10 days of the 1989 earthquake. With the possible exception of these two earthquakes, the temporal variations in seismicity (fig. 7) show no obvious precursory patterns in the 20-year period before the Loma Prieta earthquake.

A detailed examination of the hypocenters and fault-plane solutions of the events in this cluster after the 1988 Lake Elsman main shock provides clues on the nature and geometry of slip associated with these events. Fault-plane solutions for the 1988 and 1989 Lake Elsman main shocks

(events 1 and 6, respectively, fig. 9) and for the three largest 1989 aftershocks of M≥3 (events 7, 10, 18, fig. 9) were nearly identical, with oblique strike- and reverse-slip components. These five events form an alignment that approximates the strike of the main shocks' nodal planes of N. 58° W., suggesting that this alignment corresponds to the slip plane. We note that the M=4.0 event in 1981 and an M=4.5 event in 1982 (km 39 and 54, respectively, figs. 4A, 6B, 7)) occurred along an extension of this alignment and have similar fault-plane solutions (Olson, 1990). This inferred slip plane dips 60° and 66° NE. in fault-plane solutions for the 1988 and 1989 Lake Elsman main shocks, respectively, in the opposite direction from the 70° SW.-dipping plane of the Loma Prieta main shock (for example, Oppenheimer, 1990). The alignment of these M≥3 events, their focal depths, and their fault-plane solutions are consistent with slip on a northeast-dipping structure. Alternatively, but in our view less likely, these events could involve dominantly sinistral slip on a series of northeast-striking faults that form a distributed, conjugate set to the adjacent San Andreas and Sargent faults. In any case, it seems unlikely that these events involved slip on the Sargent fault, which dips steeply southwest in this area (McLaughlin, 1974).

Two cross sections of events in the Lake Elsman alignment perpendicular to the N. 58° W.-striking plane of the main-shock fault-plane solutions are shown in figures 9A and 9B. These cross sections show that most of the Lake Elsman aftershocks are located in the hanging-wall block above and within 3 km of the northeast-dipping slip plane common to the two Lake Elsman earthquakes. Of the 16 M≥1.5 aftershocks through September 1989, 13 have fault-plane solutions that are consistent with oblique strike slip and reverse slip, pure strike slip, or pure reverse slip on northwest-striking planes (figs. 9A, 9B). These fault-plane solutions and their hypocentral locations are consistent with slip on subparallel planes within the hanging-wall block. We note, however, that location errors could contribute to the scatter of these hypocenters.

Elsewhere, isolated clusters of epicenters scattered throughout the southern Santa Cruz Mountains north of the Loma Prieta main shock emphasize that deformation continues in the crust on either side of the San Andreas fault trace, consistent with geologic evidence for Quaternary displacement along range-front thrust faults, such as the Monte Vista, Berrocal, and Shannon faults (McLaughlin, 1974).

DISCUSSION

ACTIVE STRUCTURES IN THE SOUTHERN SANTA CRUZ MOUNTAINS

Whether the southwest-dipping part of the Loma Prieta rupture below 10-km depth coincided with the San Andreas fault, in which case the San Andreas fault has a listric geometry, or whether it involved a separate fault that intersects the

EXPLANATION
MAGNITUDES

· ≥0.0
·· ≥1.0
· ≥2.0
○ ≥3.0
○ ≥3.5
□ ≥4.0
□ ≥4.5
☆ ≥5.0
☆ ≥5.5
☆ ≥7.0
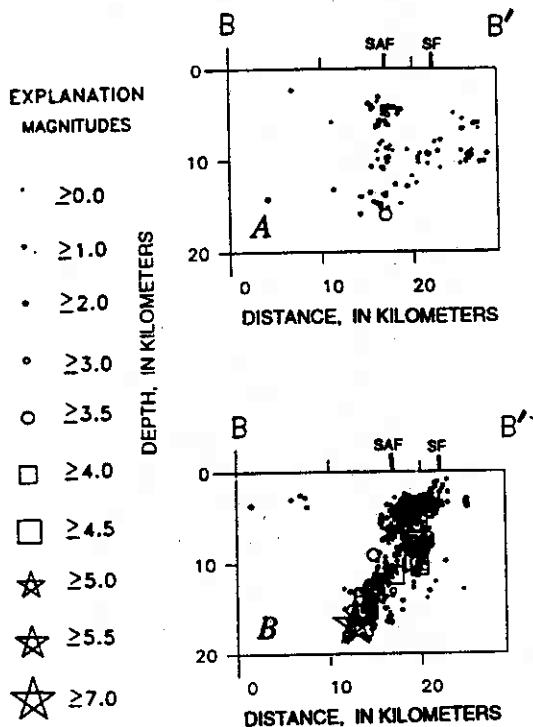
Figure 8.—Cross sections in zone B–B' (km 40–50, fig. 4) perpendicular to the San Andreas fault trace of (A) pre-earthquake events and (B) aftershocks. SAF, San Andreas fault; SF, Sargent fault.
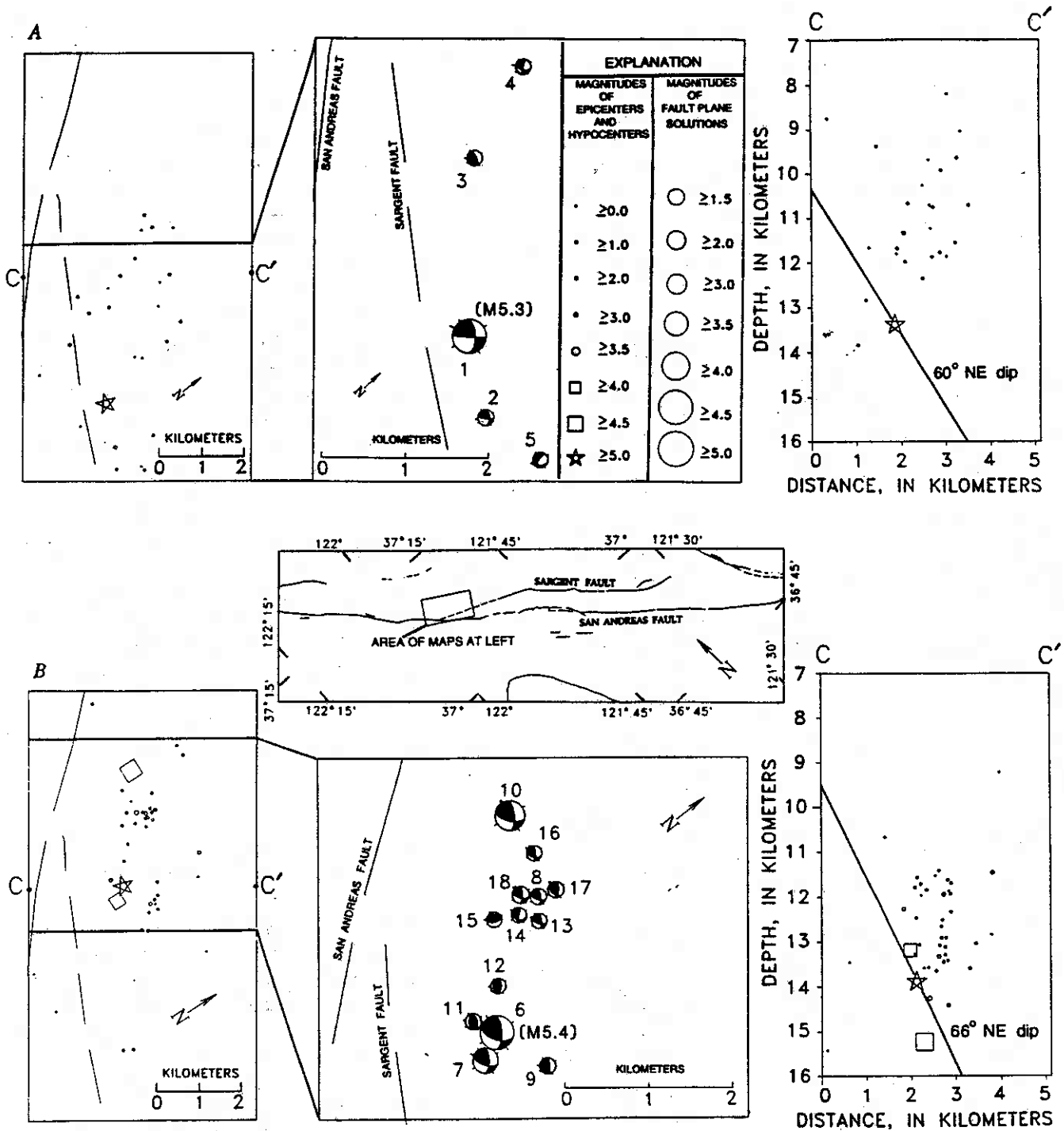
Figure 9.—Lake Elsman area (inset), showing locations of epicenters and fault-plane solutions (for M≥1.5 events) and cross sections for earthquakes between (A) time of June 27, 1988 (G.m.t.), Lake Elsman (M=5.3) main shock up to time of August 8, 1989 (G.m.t.), Lake Elsman main shock and (B) time of 1989 Lake Elsman main shock up to time of Loma Prieta main shock (fault-plane solutions are shown only for events through September). Hypocenters in cross sections are projected onto a plane through line C–C' that is perpendicular to main shocks' nodal planes striking N. 58° W., and those nodal planes' dips of 60° and 66° NE. are shown, projected through each main-shock hypocenter. C, First-motion data for fault-plane solutions shown in figures 9A and 9B, with corresponding numbers. Plusses, compressional first motion; circles, dilatational first motion; P, principal axis of compression; T, principal axis of extension. Headings list year/month/day and hour/minute (G.m.t.); M, magnitude (see text); Z, depth (in kilometers). Fault lines: solid, well located; dashed, approximately located or inferred; dotted, concealed by younger rocks or by lakes or bays.

San Andreas fault at about 10-km depth remains a matter of discussion (Dietz and Ellsworth, 1990; Olson, 1990). The few events between 10- and 16-km depth directly beneath the San Andreas fault trace and east of the main-shock hypocenter could be produced by either (1) the San Andreas fault, in which case the Loma Prieta rupture below 10-km depth involved a separate fault; or (2) discontinuous faults to the east of a southwest-dipping San Andreas fault, as Ellsworth and others (1990) suggested. In either case, several adjacent faults in the southern Santa Cruz Mountains clearly accommodate both strike-slip motion and a small component of

crustal convergence. This complex system of interacting faults reflects a combination of the broad restraining bend that the San Andreas fault forms in the study area, the triple junction formed by the intersection of the San Andreas and Calaveras faults to the south, and regional transpression common to the entire San Francisco Bay region (Aydin and Page, 1984; Harbert and Cox, 1989; Harbert, 1991).

One notable aspect of both the preearthquake and aftershock hypocenters is the broad, U-shaped distribution defined by the deepest events in both time periods that spans a zone at least 10 km wide. This depth distribution, which was first noted by Moths and others (1981) and Lindh and others (1982) for seismicity between 1969 and 1981, was one line of evidence they used to suggest that the southern Santa Cruz Mountains section of the San Andreas fault zone was likely to produce a large earthquake. Relative locations of preearthquake events and aftershocks in our study, however, show that the preearthquake events forming this U-shaped depth distribution are located northeast of the principal, southwest-dipping section of the Loma Prieta aftershock zone below about 10-km depth. Thus, this depth distribution is apparently related to crustal properties that span the 10-km width of the fault zone, rather than to properties limited to a particular fault plane. For example, maximum earthquake focal depths along the strike of the fault zone may be related in some way to the relatively high P-wave velocities calculated across the zone in three-dimensional velocity models (Eberhart-Phillips and others, 1990; Lees, 1990; Foxall and others, 1991). Foxall and others (1991) interpreted these high-velocity rocks as either upthrusted gneissic or ultramafic subcrustal rocks.

PREVIOUS $M \geq 5$ EARTHQUAKES ALONG THE LOMA PRIETA RUPTURE ZONE

The Lake Elsman earthquakes stand out against the background seismicity for the 20-year period before the Loma Prieta earthquake because they are the only $M \geq 5$ earthquakes along the rupture zone in that period and they occurred within 16 and 2½ months beforehand (see fig. 7). They also are unusual because they are a full unit of magnitude larger than the preceding events in this spatial cluster within this time period. An examination of the catalogs by Bolt and Miller (1975) and Toppozada and others (1978) reveals that only one documented $M \geq 5.0$ event since 1910 occurred within a 15-km radius of the 1988 and 1989 Lake Elsman earthquakes: an $M_L = 5.5$ earthquake on November 9, 1914 (see fig. 2), as described Townley and Allen (1939):

VIII. Santa Cruz Mountains. From reports received and from field investigations, Carl H. Beal determined the epicenter of this earthquake to have been near the small town of Laurel, Santa Cruz Co., near the crest of the Santa Cruz Mountains and about seven miles south of Los Gatos. Laurel is a mile southwest of the San Andreas fault. At Laurel two chimneys were broken off, clocks were stopped, and plaster cracked * * *. The shock was felt * * * at distances of about 100 miles, indicating a shaken area of approximately 30,000 square miles.
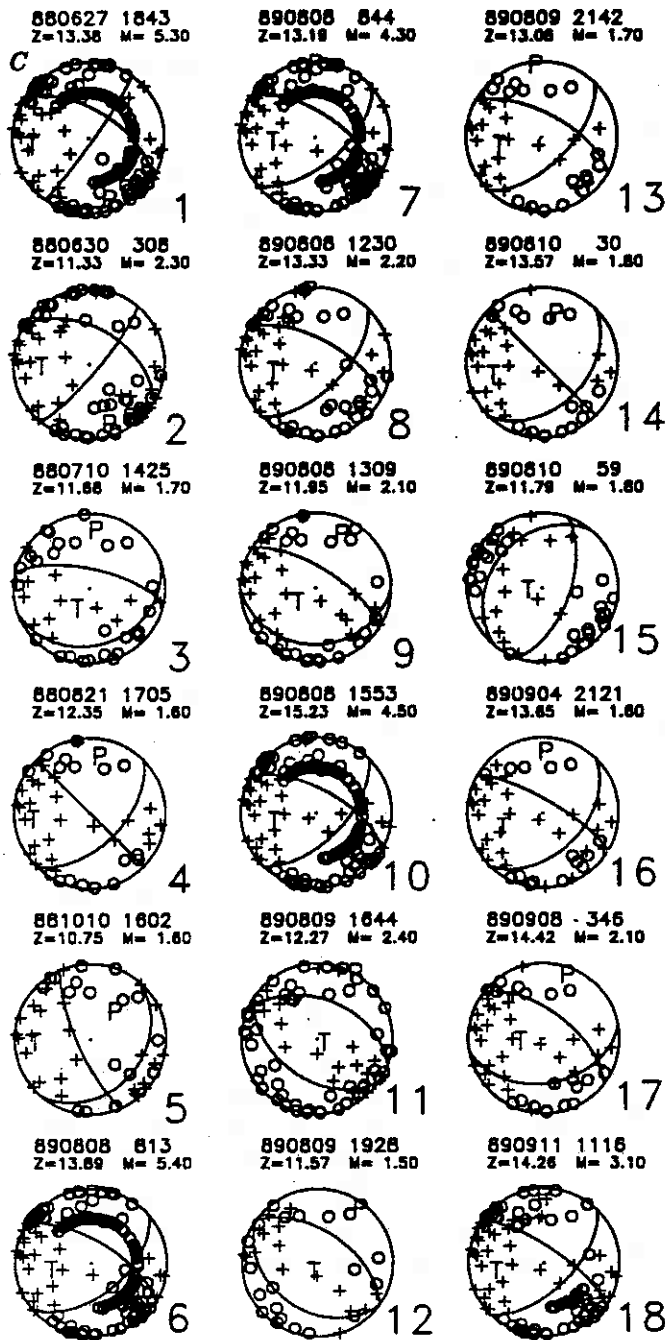

Figure 9.—Continued.

Although this event may be considered an aftershock of the 1906 earthquake and evidently produced the highest intensities near the San Andreas fault near Laurel, it need not have occurred on the San Andreas fault itself. It could, for example, have occurred on the same structure that produced the Lake Elsman earthquakes. Thus, the record of moderate earthquakes since 1910 indicates that the structure that produced the Lake Elsman earthquakes had not produced $M≥5.0$ events since at least 1914, or within the past 74 years.

Five other $M≥5$ earthquakes since 1910 may also have occurred along the Loma Prieta rupture zone, east and southeast of the main shock. Only two of these earthquakes, however, have epicenters located well enough to be associated with that zone to some degree of certainty (within ~10 km): the 1964 ($M=5.0$) and 1967 ($M=5.3$) Corralitos earthquakes. A relocation of the 1964 earthquake (McEvilly, 1966) suggests that it was associated with the same structure which produces seismicity along and northeast of the south end of the Sargent fault. The 1967 epicenter, however, is apparently located farther to the southwest and closer to the San Andreas fault trace. Thus, four moderate ($M=5$) earthquakes apparently occurred along the Loma Prieta rupture zone within the preceding 25 years.

SUMMARY

1. Well-located earthquakes in the study area since 1969 and before the Loma Prieta earthquake define conspicuous alignments along the creeping section of the San Andreas fault south of Pajaro Gap, along and east of the Sargent fault, and along the Busch Ranch and Calaveras faults. In addition, a cluster of events occurred along and east of a 10-km-long section of the Sargent fault where it intersects the San Andreas fault. The events along and east of the Sargent fault apparently are not associated with that fault, which dips steeply southwest. The events near the north end of the Sargent fault include the 1988 ($M=5.3$) and the 1989 ($M=5.4$) Lake Elsman earthquakes, located 10 and 12 km, respectively, north-northeast of the Loma Prieta main shock. Elsewhere, a few events occurred along the 35-km-long section of the San Andreas fault trace between Pajaro Gap and Lake Elsman, and isolated events occurred on both sides of the San Andreas fault trace throughout the southern Santa Cruz Mountains north of the Loma Prieta main shock.

2. Fault-plane solutions for both the 1988 and 1989 Lake Elsman main shocks show oblique strike slip and reverse slip on a plane that strikes N. 58° W. and dips 60°–66° NE., suggesting that these earthquakes may have occurred on a common, blind fault. Fault-plane solutions and hypocenters for most of the Lake Elsman aftershocks ($M≥1.5$) are consistent with oblique slip in the hanging-wall block on planes subparallel to the inferred slip plane common to the 1988 and 1989 Lake Elsman main shocks.

3. The Lake Elsman earthquakes are unusual even though they occurred within an area of persistent background seismicity, because they were a full unit of magnitude larger than all other events recorded within a 15-km radius during the preceding 74 years, because they are the only $M≥5$ events in the 20-year period before the Loma Prieta earthquake located along the rupture zone, and because they occurred within 16 and 2½ months beforehand. Two other $M≥5$ earthquakes since 1960, however, also occurred along the rupture zone: the 1964 ($M=5.0$) and 1967 ($M=5.3$) Corralitos earthquakes, located approximately 17 km east and 10 km southeast, respectively, of the Loma Prieta main shock. Given location errors greater than 10 km for earthquakes before 1960 in the southern Santa Cruz Mountains, other $M≥5$ events may have occurred along the rupture zone since 1910, including those in 1910 ($M=5.5$), 1914 ($M=5.5$), 1954 ($M=5.3$) and 1959 ($M=5.3$).

4. The southwest-dipping section of the Loma Prieta rupture zone beneath 10-km depth produced virtually no microseismicity for at least 20 years before the Loma Prieta earthquake.

5. The hypocenters of earthquakes occurring in the study area since 1969 form a broad U-shaped distribution when projected onto a vertical plane parallel to the San Andreas fault trace. This depth distribution of preearthquake seismicity approximately forms a lower bound to the distribution of Loma Prieta aftershocks, even though the events below 10-km depth both before and after the earthquake occurred on different fault planes within the 10-km-wide zone.

REFERENCES CITED

Anderson, R.S., 1990, Evolution of the northern Santa Cruz Mountains by advection of crust past a San Andreas fault bend: Science, v. 249, no. 4967, p. 397–401.

Aydin, Atilla, and Page, B.M., 1984, Diverse Pliocene-Quaternary tectonics in a transform environment, San Francisco Bay region, California: Geological Society of America Bulletin, v. 95, no. 11, p. 1303–1317.

Beroza, G.C., 1991, Near-source modeling of the Loma Prieta earthquake; evidence for heterogeneous slip and implications for earthquake hazard: Seismological Society of America Bulletin, v. 81, no. 5, p. 1603–1621.

Bolt, B.A., and Miller, R.D., 1975, Catalog of earthquakes in northern California and adjoining areas, 1 January 1930–31 December 1972: Berkeley, University of California, Seismographic Station, 567 p.

Burford, R.O., and Harsh, P.W., 1980, Slip on the San Andreas fault in central California from alinement array surveys: Seismological Society of America Bulletin, v. 70, no. 4, p. 1233–1261.

Dietz, L.D., and Ellsworth, W.L., 1990, The October 17, 1989 Loma Prieta, California, earthquake and its aftershocks; geometry of the sequence from high-resolution locations: Geophysical Research Letters, v. 17, no. 9, p. 1417–1420.

Eaton, J.P., 1989, Dense microearthquake network study of northern California earthquakes, chap. 13 *of* Litehiser, J.J., ed., Observatory seismology, a centennial symposium for the Berkeley Seismographic Stations: Berkeley, University of California Press, p. 199–224.

———1992, Determination of amplitude and duration magnitudes and site residuals from short-period seismographs in northern California: Seismological Society of America Bulletin, v. 82, no. 2, p. 533–579.

Eaton, J.P., Lee, W.H.K., and Pakiser, L.C., 1970, Use of microearthquakes in the study of the mechanics of earthquake generation along the San Andreas fault in central California: Tectonophysics, v. 9, no. 2–3, p. 259–282.

Eberhart-Phillips, Donna, Labson, V.F., Stanley, W.D., Michael, A.J., and Rodriguez, B.D., 1990, Preliminary velocity and resistivity models of the Loma Prieta earthquake region: Geophysical Research Letters, v. 17, no. 8, p. 1235–1238.

Ellsworth, W.L., 1990, Earthquake history, 1769–1989, chap. 6 *of* Wallace, R.E., ed., The San Andreas fault system, California: U.S. Geological Survey Professional Paper 1515, p. 153–188.

Ellsworth, W.L., Dietz, L.D., and Lindh, A.G., 1990, Accommodation of North America-Pacific plate motion along the Loma Prieta earthquake rupture zone; where is the real San Andreas fault? [abs.]: Eos (American Geophysical Union Transactions), v. 71, no. 43, p. 1646.

Foxall, William, Michelini, Alberto, and McEvilly, T.V., 1991, Structure and fault processes of the Loma Prieta earthquake from a three-dimensional P-velocity model [abs.]: Eos (American Geophysical Union Transactions), v. 72, no. 44, supp., p. 311.

Harbert, William, 1991, Late Neogene relative motions of the Pacific and North American Plates: Tectonics, v. 10, no. 1, p. 1–15.

Harbert, William, and Cox, Allan, 1989, Late Neogene motion of the Pacific Plate: Journal of Geophysical Research, v. 94, no. B3, p. 3052–3064.

Hill, D.P., Eaton, J.P., and Jones, L.M., 1990, Seismicity, 1980–86, chap. 5 *of* Wallace, R.E., ed., The San Andreas fault system, California: U.S. Geological Survey Professional Paper 1515, p. 115–152.

Hill, D.P., Eaton, J.E., Ellsworth, W.L., Cockerham, R.S., Lester, F.W., and Corbett, E.J., 1991, The seismotectonic fabric of central California, *in* Slemmons, D.B., Engdahl, E.R., Blackwell, D.D., Schwartz, D.P., and Zoback, M.D., eds., Neotectonics of North America (DNAG Associated Volume GSMV–1): Boulder, Colo., Geological Society of America, p. 107–132.

Irwin, W.P., 1990, Geology and plate-tectonic development, chap. 3 *of* Wallace, R.E., ed., The San Andreas fault system, California: U.S. Geological Survey Professional Paper 1515, p. 61–82.

King, G.C.P., Lindh, A.G., and Oppenheimer, D.H., 1990, Seismic slip, segmentation, and the Loma Prieta earthquake: Geophysical Research Letters, v. 17, no. 9, p. 1449–1452.

Klein, F.W., 1989, User's guide to HYPOINVERSE, a program for VAX computers to solve earthquake locations and magnitudes: U.S. Geological Survey Open-File Report 89–314, 58 p.

Lee, W.H.K., and Stewart, S.W., 1981, Principles and applications of microearthquake networks: New York, Academic Press, 293 p.

Lees, J.M., 1990, Tomographic P-wave velocity images of the Loma Prieta earthquake asperity: Geophysical Research Letters, v. 17, no. 9, p. 1433–1436.

Lindh, A.G., Moths, B.L., Ellsworth, W.L., and Olson, J.A., 1982, Historic seismicity of the San Juan Bautista, California region [abs.], *in* Hill, D.P., and Nishimura, Keiji, chairmen, U.S.-Japan Conference on Natural Resources (UJNR), Panel on Earthquake Prediction Technology Joint Meeting, 2d, Menlo Park, Calif., 1981, Proceedings: U.S. Geological Survey Open-File Report 82–180, p. 45–50.

Lisowski, Michael, Prescott, W.H., Savage, J.C., and Johnston, M.J.S., 1990, Geodetic estimates of coseismic slip during the 1989 Loma Prieta, California earthquake: Geophysical Research Letters, v. 17, no. 9, p. 1437–1440.

McEvilly, T.V., 1966, The earthquake sequence of November 1964 near Corralitos, California: Seismological Society of America Bulletin, v. 56, no. 3, p. 755–773.

McLaughlin, R.J., 1974, The Sargent-Berrocal fault zone and its relation to the San Andreas fault system in the southern San Francisco Bay region and Santa Clara Valley, California: U.S. Geological Survey Journal of Research, v. 2, no. 5, p. 593–598.

Moths, B.L., Lindh, A.G., Ellsworth, W.L., and Fluty, L., 1981, Comparison between the seismicity of the San Juan Bautista and Parkfield regions, California [abs.]: Eos (American Geophysical Union Transactions), v. 62, p. 958.

Olson, J.A., 1990, Seismicity in the twenty years preceding the 1989 Loma Prieta, California earthquake: Geophysical Research Letters, v. 17, no 9, p. 1429–1432.

Oppenheimer, D.H., 1990, Aftershock slip behavior of the 1989 Loma Prieta, California earthquake: Geophysical Research Letters, v. 17, no. 8, p. 1199–1202.

Pavoni, N., 1973, A structural model for the San Andreas fault zone along the northeast side of the Gabilan Range, *in* Kovach, R.L., and Nur, Amos, eds., Proceedings of the conference on tectonic problems of the San Andreas fault system: Stanford, Calif., Stanford University Publications in the Geological Sciences, v. 13, p. 259–267.

Reasenberg, Paul, and Oppenheimer, D.H., 1985, FPFIT, FPPLOT, and FPPAGE, FORTRAN computer programs for calculating and displaying earthquake fault-plane solutions: U.S. Geological Survey Open-File Report 85–739, 109 p.

Rogers, T.H., 1980, Geology and seismicity at the convergence of the San Andreas and Calaveras fault zones near Hollister, San Benito County, California, *in* Streitz, Robert, and Sherburne, R.W., eds., Studies of the San Andreas fault zone in northern California: California Division of Mines and Geology Special Report 140, p. 19–28.

Schulz, S.S., Mavko, G.M., Burford, R.O., and Stuart, W.D., 1982, Long-term fault creep observations in central California: Journal of Geophysical Research, v. 87, no. B8, p. 6977–6982.

Seeber, Leonardo, and Armbruster, J.G., 1990, Fault kinematics in the 1989 Loma Prieta rupture area during 20 years before that event: Geophysical Research Letters, v. 17, no. 9, p. 1425–1428.

Segall, Paul, and Lisowski, Michael, 1990, Surface displacements in the 1906 San Francisco and 1989 Loma Prieta earthquakes: Science, v. 250, no. 4985, p. 1241–1244.

Spieth, M.A., 1981, Two detailed seismic studies in central California. Part I: Earthquake clustering and crustal structure studies of the San Andreas fault near San Juan Bautista. Part II: Seismic velocity structure along the Sierra foothills near Oroville, California: Stanford, Calif., Stanford University, Ph.D. thesis, 174 p.

Steidl, J.H., Archuleta, R.J., and Hartzell, S.H., 1991, Rupture history of the 1989 Loma Prieta, California earthquake: Seismological Society of America Bulletin, v. 81, no. 5, p. 1573–1602.

Thatcher, Wayne, 1990, Present-day crustal movements and the mechanics of cyclic deformation, chap. 7 *of* Wallace, R.E., ed., The San Andreas fault system, California: U.S. Geological Survey Professional Paper 1515, p. 153–188.

Toppozada, T.R., Parke, D.L., and Higgins, C.T., 1978, Seismicity of California, 1900–1931: California Division of Mines and Geology Special Report 135, 39 p.

Townley, S.D., and Allen, M.W., 1939, Descriptive catalog of earthquakes of the Pacific coast of the United States, 1769 to 1928: Seismological Society of America Bulletin, v. 29, no. 1, p. 1–297.

Valensise, Gianluca, and Ward, S.N., 1991, Long-term uplift of the Santa Cruz coastline in response to repeated earthquakes along the San Andreas fault: Seismological Society of America Bulletin, v. 81, no. 5, p. 1694–1704.

Wald, D.J., Helmberger, D.V., and Heaton, T.H., 1991, Rupture model of the 1989 Loma Prieta earthquake from the inversion of strong motions and broadband teleseismic data: Seismological Society of America Bulletin, v. 81, no. 5, p. 1540–1572.

THE LOMA PRIETA, CALIFORNIA, EARTHQUAKE OF OCTOBER 17, 1989:
EARTHQUAKE OCCURRENCE

PRESEISMIC OBSERVATIONS

ANALYSIS OF LOW-FREQUENCY-ELECTROMAGNETIC-FIELD MEASUREMENTS NEAR THE EPICENTER

By Anthony C. Fraser-Smith, Arman Bernardi,[1] Robert A. Helliwell, Paul R. McGill, and O.G. Villard, Jr.,
Stanford University

CONTENTS

ABSTRACT

We summarize the results of measurements of low-frequency electromagnetic fields by two independent monitoring systems before the earthquake. Taken together, these measurements cover 25 narrow frequency bands in the more than six-decade frequency range 0.01 Hz–32 kHz, with a time resolution ranging from half an hour in the ultra-low-frequency (ULF) range (0.01–10 Hz) to 1 s in the extremely low frequency/very low frequency (ELF/VLF) range (10 Hz–32 kHz). The ULF system is located near Corralitos, Calif., about 7 km from the epicenter, and the ELF/VLF system on the Stanford University campus, about 52 km from the epicenter. As previously reported, analysis of these ELF/VLF data has revealed no precursory activity, although the ULF data have some distinctive and anomalous features. First, a narrow-band signal in the range 0.05–0.2 Hz appeared about September 12 and persisted until the appearance of a second anomalous feature, which consisted of a substantial increase in the noise background starting on October 5 that covered almost the entire frequency range of the ULF system but was greatest at the lowest frequencies. Third, there was an anomalous dip in the noise background in the range 0.2–5 Hz starting 1 day before the earthquake. Finally and, possibly, most

[1] Current affiliation: Teknekron Communications Systems, Berkeley, CA 94704.

compelling, there was an increase to an exceptionally high level of activity in the range 0.01–0.5 Hz (that is, at the lowest frequencies) starting approximately 3 hours before the earthquake. There do not appear to have been any magnetic-field fluctuations originating in the upper atmosphere that can account for this increase. Furthermore, although the measurement systems are sensitive to motion, seismic measurements indicate no significant shocks before the earthquake. Thus, the various anomalous features in the data, particularly the large-amplitude increase in activity starting 3 hours before the earthquake, may have been magnetic precursors. The observation of the largest magnetic-field amplitudes at the lowest frequencies, and the absence of ELF/VLF signals, suggest that the anomalous signals may have originated in the hypocentral region and propagated to the surface. If so, modeling with electric- and magnetic-dipole sources further suggests that the ULF signals could have been detected at the surface as far as 100 km from the epicenter.

INTRODUCTION

At 5:04 p.m. P.d.t. October 17, 1989 (0004:15.24 G.m.t. Oct. 18), a moderately large (M_S=7.1) earthquake occurred "suddenly and without foreshock activity" in northern California (U.S. Geological Survey staff, 1990). Its epicenter (lat 37.039° N., long 121.879° W.) was located near Loma Prieta, one of the highest peaks in the California Coast Ranges, just south of the San Francisco Bay region (fig. 1). At the time of the earthquake, we were operating two independent electromagnetic-noise-monitoring systems at locations relatively close to the epicenter, in continuation of a program of low-frequency-radio-noise measurements that has been in progress for several years. Taken together, these two systems provided complete coverage of magnetic-field changes over the broad frequency range from 0.01 Hz to 32 kHz. One, an ultra-low-frequency (ULF) system (0.01–10 Hz), was located at Corralitos, Calif. (lat 37.015° N., long 121.806° W.), only 7 km from the epicenter; and the other, an extremely low/very low frequency (ELF/VLF)

system (0.01 Hz–32 kHz), was located on the Stanford University campus (lat 37.43° N., long 122.18° W.), about 52 km from the epicenter (fig. 1).

We began analyzing the data from our ELF/VLF measurement system immediately after the earthquake in expectation of seeing precursory signals, because there have been many reports in recent years of possible ELF/VLF electromagnetic precursors to earthquakes (for example, Gokhberg and others, 1981, 1982b; Oike and Ogawa, 1982; Parrot and Mogilevsky, 1989; Tate and Daily, 1989; Larkina and others, 1983, 1989; Serebryakova and others, 1992). Somewhat later, when contact was reestablished with the Corralitos system, we began processing the ULF data from that location. We had less reason to expect electromagnetic precursors in those data because previous reports of precursory signals at frequencies below the ELF/VLF range have, with few exceptions, involved frequencies below our ULF range of operation (for example, Rikitake, 1975, p. 207–209; Shapiro and Abdullabekov, 1982; Johnston, 1989; Varotsos and Lazaridou, 1991). As we subsequently reported (Fraser-Smith and others, 1990a, b), we were unable to detect any precursory changes in the Stanford University ELF/VLF data. Although there were some small changes in these data during the days before the earthquake (in addition to their diurnal variation), similar small changes are commonly observed at other times, and so they must be considered a normal feature of the data. The Corralitos ULF data, however, contained several anomalous features that may prove to be precursors (Fraser-Smith and others, 1990a, b; Bernardi and others, 1991).

In the following sections, we summarize previously published results, consisting primarily of descriptions of our equipment and preearthquake measurements, as well as some new results that support and extend this earlier work. In addition, we perform some simple, general modeling of the measured ULF magnetic fields, assuming both electric- and magnetic-dipole sources, to obtain an order-of-magnitude estimate of the range of distances over which these fields can be detected.

ELF/VLF MEASUREMENTS

The Stanford University ELF/VLF electromagnetic-noise-monitoring system is one of eight identical instruments that have been installed around the world as part of a global survey of ELF/VLF radio noise (Fraser-Smith and Helliwell, 1985; Fraser-Smith and others, 1988, 1991). Crossed-loop antennas are used to measure the magnetic component of the noise. This system records both analog and digital data and computes, in real time, various statistical quantities that define the characteristics of the noise and that can be further processed to provide additional statistical measures of it. The data of immediate interest to us are the average amplitudes that are computed at the end of every minute from 600 measurements at a rate of 10 samples per second on the envelope of the signal emerging from 16 narrow-band (5-percent bandwidth) filters, the center frequencies of which are at 10, 30, 80, 135, 275, 380, 500, and 750 Hz and 1.0, 1.5, 2.0, 3.0, 4.0, 8.0, 10.2, and 32.0 kHz.

Many different plots of the 1-minute-average noise amplitudes for the month before the earthquake were prepared and analyzed. However, as described by Fraser-Smith and others (1990a, b), when account was taken of normal variations in the ELF/VLF noise data, no unusual changes in the amplitudes were distinguishable at any time before the earthquake. To illustrate the form of the data, Fraser-Smith and others (1990a) showed simultaneous plots of the 1-minute averages for 10 Hz, 500 Hz, 2 kHz, and 8 kHz for the 8-day interval October 13–20, 1989. This presentation is expanded in figure 2, which shows simultaneous plots of the 1-minute averages for 135 Hz, 380 Hz, 1 kHz, and 4 kHz for the same 8-day interval. Once again, the only obvious features are the mostly well-defined diurnal variations that persist essentially unchanged throughout this interval. Commonly, small changes, sometimes referred to as "glitches," are noticeable in the data; however, because these small changes are natural, they are indistinguishable from any signals that might be precursors to the earthquake.

Fraser-Smith and others (1990a) also pointed out that a negative result is not completely unexpected, because on
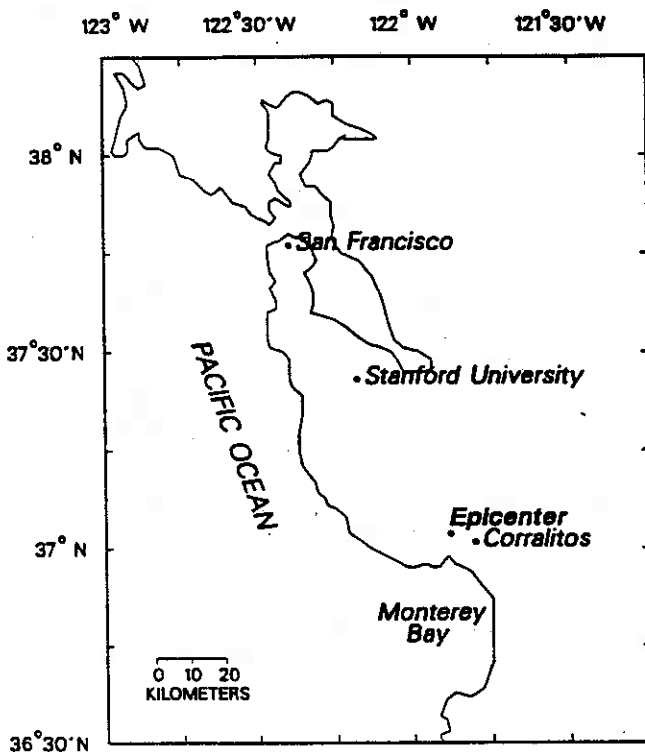

Figure 1.—San Francisco Bay region, showing locations of epicenter of Loma Prieta earthquake and of Corralitos and Stanford University noise-monitoring systems.

three earlier occasions unsuccessful searches had been made for precursory signals in the Stanford University ELF/VLF noise data after local earthquakes of $M\sim5$ (Alum Rock, June 13, 1988, $M_L=5.3$; Lake Ellsman 1, June 27, 1988, $M_L=5.0$; Lake Ellsman 2, August 8, 1989, $M_L=5.2$). Since the publication of these negative results, an extensive search has also been made for precursory signals in the ELF/VLF wave data obtained by the low-altitude Dynamics Explorer 2 (DE–2) satellite (apogee, ~1,300 km; perigee, ~300 km; inclination, ~90°) near the times of 60 earthquakes, but without success (Henderson and others, 1991). The results of these various studies show that measurable ELF/VLF electromagnetic precursors are not always associated with earthquakes.

ULF MEASUREMENTS

The Corralitos magnetic-field-monitoring system is one of four new models that we have built to characterize and monitor the state of natural geomagnetic activity in the ULF range 0.01–10 Hz (Bernardi and others, 1989). They are conventional in many of their technical details, including their use of solenoidal coils as sensors; however, they differ significantly from previous systems used by our laboratory and others for measurements of ULF geomagnetic-field changes, through their use of a small computer as an integral part of the measurement system and through an emphasis on the real-time computation of digital measurements of the noise power as an alternative to analog chart
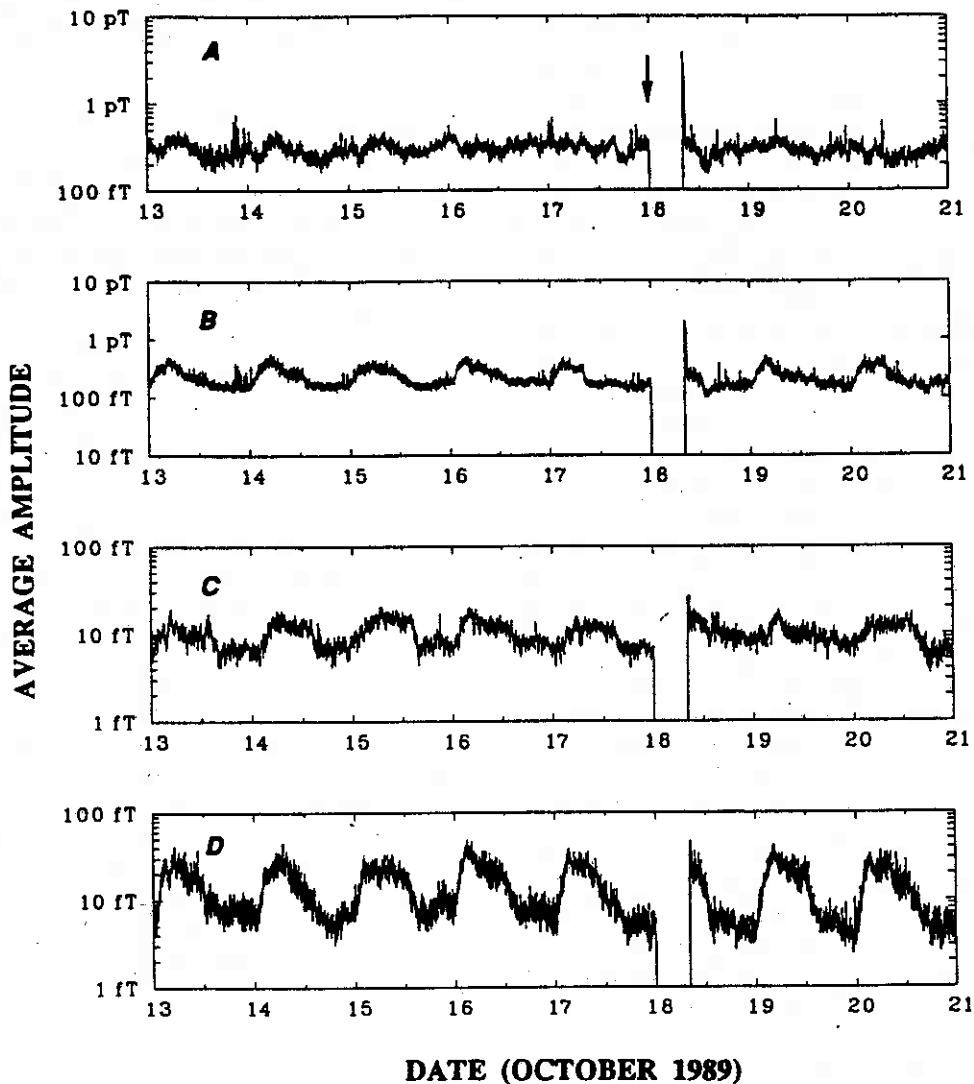
Figure 2.—1-minute-average extremely low frequency/very low frequency noise amplitudes measured during interval October 13–20, 1989, at Stanford University for frequencies of (A) 135 Hz, (B) 380 Hz, (C) 1 kHz, and (D) 4 kHz. Earthquake occurred just after 0004 G.m.t. October 18 (arrow), followed immediately by an 8-hour power failure. Large transient impulses during 1-hour period immediately after recommencement of measurements are probably related to automatic restart, instead of aftershock activity. Note different amplitude scales.

Table 1.—*Frequency ranges for which magnetic-activity (MA) indices are computed, and their center frequencies*

MA index	frequency band (Hz)	Center frequency (Hz)
MA3	0.01–0.02	0.015
MA4	.02–0.05	.033
MA5	.05–0.10	.073
MA6	.10–0.20	.150
MA7	.20–0.50	.352
MA8	.50–1.00	.751
MA9	1.00–2.00	1.502
MA10	2.00–5.00	3.501
MA11	5.00–10.0	7.500

recordings. As described in greater detail by Bernardi and others (1989), the basic output of each index-generation system is a set of logarithms to the base 2 of the half-hourly averages of the power in nine frequency bands covering the overall range 0.01–10 Hz (table 1). These logarithms compose our magnetic-activity (MA) indices, which are stored permanently on magnetic disk and are continuously available by telephone line (the raw samples were originally discarded, owing to limitations in storage capacity, but as much as about 6 days of the most recent samples is now recorded on magnetic disk in our latest models). These MA indices can be converted to conventional magnetic-field units by using a table of conversion factors (for example, Fraser-Smith and others, 1990a), and all the Corralitos ULF data presented here were derived from MA indices by using these conversion factors.

The Corralitos index generator has been in operation since October 1987. It was running during the Alum Rock and Lake Ellsman 2 earthquakes discussed in the preceding section, but its measurements showed no evidence of precursory signals. As already noted, its location was fortuitously only 7 km from the epicenter of the Loma Prieta earthquake. There was a 39-hour loss of power after the earthquake, after which, when power was restored, the system automatically recommenced operation. When the MA indices were inspected, there clearly had been major changes in the measurements not only during the few hours before the earthquake but also during the preceding weeks.

As originally described by Fraser-Smith and others (1990a), we first suspected that the anomalous changes observed before the earthquake could have been caused either by precursory seismic activity moving the coil sensor and generating spurious signals, or by an extraordinarily lengthy interval of natural large-amplitude magnetic activity. Because of the half-hour averaging involved in their computation, MA indices are not particularly sensitive to even moderately large ground motions of short duration (local earthquakes of M–5 have caused only small coseismic increases in the indices), and so the seismic activity

required to cause these anomalous changes must have been either particularly persistent, very strong, or both. However, we were able to establish that no significant seismic activity had occurred before the earthquake (W.L. Ellsworth and M.J.S. Johnston, oral and written communs., 1989; U.S. Geological Survey staff, 1990). In addition, the available MA indices showed no evidence of magnetic storms or other increases in geomagnetic activity that could account for our measurements before the earthquake. (The daily sum of Kp remained less than 27+ throughout the interval October 1–19; there was a moderately large storm on October 20–21, when the sum of Kp reached 57). These considerations, in combination with the results of the more extensive study by Bernardi and others (1991), lead us to conclude that the anomalous magnetic-field fluctuations were probably not caused either by precursory seismic activity or by naturally occurring magnetic-field activity originating in the upper atmosphere.

The complete set of MA indices for the months of September and October 1989 are plotted in figure 2 of Fraser-Smith and others (1990a) and in figures 2 and 3 of Bernardi and others (1991). Four anomalous changes in MA indices were identified by these investigators, the first starting around September 12, when unusual bursts of activity began to appear in the data for the two adjacent frequency bands 0.05–0.1 and 0.1–0.2 Hz. The signal generating these changes increased in amplitude until it reached a peak of about 1.5 nT, and the unusual alternation of its amplitude between the two frequency bands suggested that the signal had a narrow bandwidth centered on 0.1 Hz and that this center frequency drifted between the two bands (Bernardi and others, 1991). On October 5, the narrow-bandwidth signal disappeared upon the occurrence of the second anomalous change in the measurements: a large and sustained increase in the noise background covering all the frequencies of operation but strongest at the lowest frequencies (–0.01 Hz), where the amplitude increased to about 30 times the normal background amplitude. This noise background gradually declined in strength until the day before the earthquake, when the third and fourth anomalous changes occurred. The third anomalous change was a distinctive drop and recovery in the noise background in the frequency range 0.2–5 Hz, and the fourth anomalous change, confined to the frequency range 0.01–0.5 Hz, was an increase to an exceptionally high level of activity starting approximately 3 hours before the earthquake.

The changes that occurred at 0.01 Hz just before the earthquake are plotted in figure 3, in the same format as figure 3 of Fraser-Smith and others (1990a). Absolute magnetic field units are used, and we note that the largest amplitudes measured during the 3-hour period before the earthquake exceed the already-enhanced levels on October 16–17 by a factor of 10 to 30 (the amplitudes of the largest signals also exceed the dynamic range of the measure-

ment system, and so the measured amplitudes are actually smaller than the true values). The data obtained during the aftershock interval, some of which are plotted in figure 3, are of great interest, but their analysis is made difficult by the large number and variety of aftershocks, by the shaking response of the measurement system, and by the occurrence of a magnetic storm on October 20–21. Analysis of these aftershock data fails to show any correlation between the measured geomagnetic activity and the frequency or magnitude of aftershocks (Fenoglio and others, 1991, 1992).

For comparison with figure 3, the same 0.01-Hz measurements for the month of August 1989 are plotted in figure 4, which shows that the normal natural background noise is typically near 0.3 to 0.6 $nT/\sqrt{Hz}$, with occasional short-lived bursts in the range 1–10 $nT/\sqrt{Hz}$. An additional feature of these data is the absence of response to the occurrence of the $M_L=5.2$ Lake Ellsman 2 earthquake at 0814 G.m.t. August 8, the epicenter of which was less than 30 km from Corralitos.

By converting the MA indices for each of the nine adjacent narrow frequency bands into their equivalent amplitudes in magnetic-field units (for example, Fraser-Smith and others, 1990a) and then plotting amplitude against frequency for each half-hour interval, a succession of average spectra can be obtained to investigate changes in the frequency content of ULF magnetic-field fluctuations before the earthquake. A series of these spectra for the 8-hour period before the earthquake, starting at 1600 G.m.t. October 17 and ending at 0000 G.m.t. October 18, is shown in figure 5. These spectra are almost identical for the two

half-hour intervals ending at 1600 and 1800 G.m.t., but their low-frequency content then increases rapidly; the largest increase occurs during the half-hour period ending at 0000 G.m.t.—that is, just before the earthquake. This increase is greatest for frequencies in the range 0.01–0.1 Hz and almost negligible for the highest frequencies (~10 Hz), in agreement with the results of studies of the MA-index plots by Fraser-Smith and others (1990a) and Bernardi and others (1991).

Figure 4.—Magnetic-field amplitude during August 1989 at Corralitos for 0.01-Hz frequency. Fluctuations shown here can be considered typical of normal changes in natural background noise measured at Corralitos. Nevertheless, we note that $M_L=5.2$ Lake Ellsman 2 earthquake of 0814 G.m.t. August 8 occurred only a short distance away with no obvious effect on measurements. As in figure 3, amplitudes can be converted to nanoteslas by taking account of bandwidth for measurements at 0.01-Hz, which here means multiplying by $\sqrt{0.00732}$, or 0.0855.
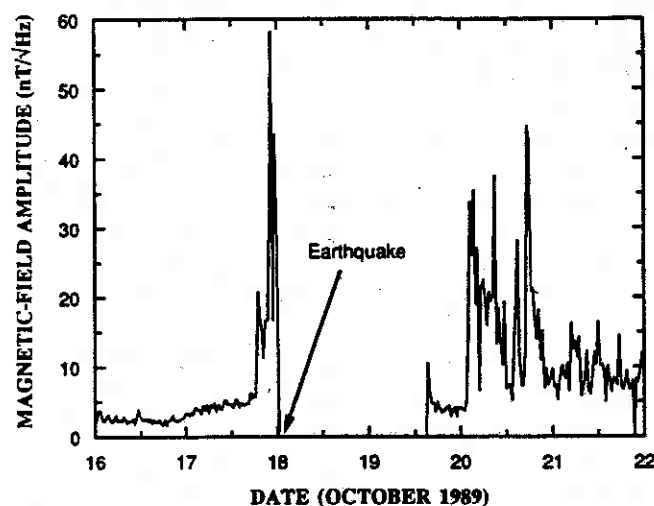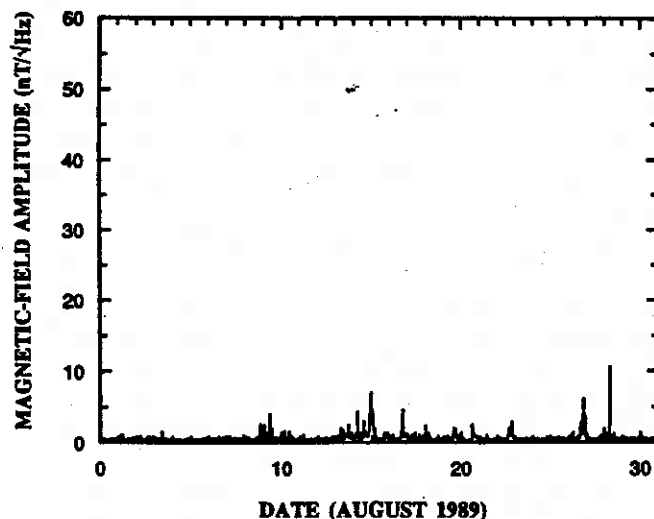
Figure 3.—Magnetic-field amplitude during interval October 16–22, 1989, at Corralitos for 0.01-Hz frequency. Earthquake occurred just after 0004 G.m.t. October 18, followed immediately by a power failure, whereupon magnetic field measurements went to zero. Large peaks after earthquake include many aftershocks, as well as a magnetic storm that peaked on October 20–21. Amplitudes can be converted to nanoteslas by taking account of bandwidth for measurements at 0.01 Hz, which here means multiplying by $\sqrt{0.00732}$, or 0.0855.
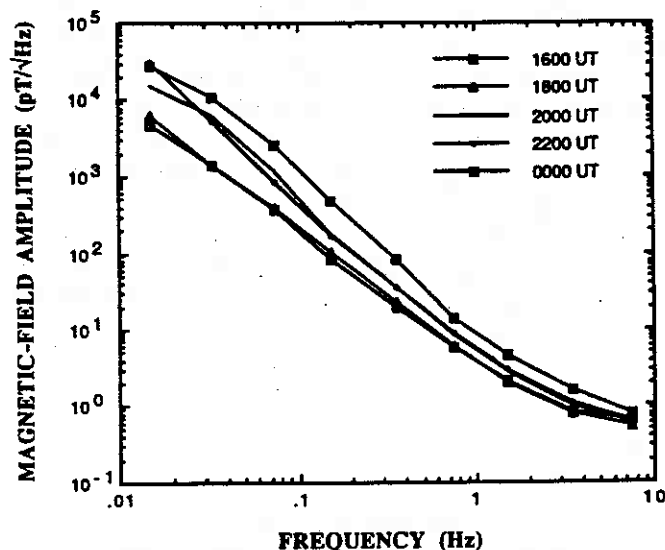
Figure 5.—Spectral variation of magnetic activity at Corralitos before Loma Prieta earthquake.

DIPOLE MODELS

There are a surprisingly large number of possible generation mechanisms for the ULF magnetic fields observed at Corralitos before the earthquake, many of which have already been used to explain or predict electric- and magnetic-field changes before and during earthquakes. Some of the most commonly evoked mechanisms involve piezomagnetic or piezoelectric effects, electrokinetic phenomena (or streaming potentials), and crustal-resistivity changes due to stress (for example, Stacey, 1964; Mizutani and others, 1976; Gokhberg and others, 1982a; Johnston, 1989). In addition, new mechanisms are still being proposed (for example, Draganov and others, 1991). Thus, the task of explaining the Corralitos ULF magnetic fields is not so much one of identifying a single mechanism as distinguishing between several competing mechanisms. We do not have the resources to study all the various mechanisms to see whether any one of them can explain the Corralitos measurements, and so we confine ourselves here to a more limited modeling effort in which we investigate the possible range of detection of the Corralitos ULF magnetic fields by applying earlier work (sponsored by the U.S. Office of Naval Research) on the low-frequency electromagnetic fields generated by submerged dipole sources.

In the following analysis, which is directed solely toward estimating the distance range over which ULF magnetic fields could have been measured, we simply assume that the source of the Loma Prieta ULF magnetic fields can be modeled by single electric- and/or magnetic-dipole sources situated in the hypocentral region. This assumption leaves open the actual mechanism of generation of these dipole sources (as indicated above, there are several possible mechanisms) and made plausible by the frequency variation of the magnetic fields. As we mentioned, we were unable to measure any precursory ELF signals at Stanford University, about 50 km from the epicenter. At Corralitos, the largest ULF amplitudes were measured at the lowest frequencies (~0.01 Hz). We now show that this variation is consistent with electric- or magnetic-dipole sources situated in the ground at depths comparable to that of the Loma Prieta hypocenter.

The attenuation of electromagnetic fields generated by electric- or magnetic-dipole sources submerged in an electrically conducting medium is well characterized by the skin depth δ, defined as

$$\delta = \sqrt{\frac{2}{\omega\mu\sigma}}, \qquad (1)$$

where ω is the angular frequency ($\omega = 2\pi f$), μ is the permeability of the medium (which we assume to be the same as the permeability of free space, μ_0, where $\mu_0 = 4\pi \times 10^{-7}$ H/m) and σ is the electrical conductivity. For a plane electromagnetic wave propagating into a conducting medium, δ is a

Table 2.—*Skin depths for various frequencies and electrical conductivities*

[All values in kilometers. Seawater generally has a conductivity close to 4 S/m, whereas typical "earth" has a conductivity in the range 0.01–0.1 S/m. The conductivity of dry rock varies widely, but a value of 0.0001 S/m is representative]

Frequency (Hz)	Conductivity (S/m)		
	10^{-4}	10^{-1}	4
10^3	1.59	0.050	0.0079
10^2	5.03	.159	.025
10	15.9	.503	.079
1	50.3	1.59	.25
10^{-1}	159	5.03	.79
10^{-2}	503	15.9	2.5
10^{-3}	1,590	50.3	7.9

measure of the distance over which the amplitude of the wave is attenuated to $1/e$ of its original value, where $e = 2.71828...$ is the usual exponential factor. The electromagnetic fields generated by a buried dipole source are not attenuated purely exponentially, as they are for a plane wave, particularly when the measurement point is close to the source (as measured in skin depths); but in most cases δ will be at least approximately representative of this distance.

The δ values for representative frequencies and electrical conductivities are listed in table 2. We note that $\delta = 15.9$ km for $f = 0.01$ Hz and $\sigma = 0.1$ S/m, which is a conservative estimate of the electrical conductivity in the Earth's surface layer (for example, Watt and others, 1963). This δ value is comparable to the estimated 17.6-km depth of the hypocenter of the Loma Prieta earthquake (U.S. Geological Survey staff, 1990), implying that electromagnetic signals with a frequency of 0.01 Hz originating near the hypocenter will be only moderately attenuated as they propagate upward to the Earth's surface. In comparison, $\delta = 1.59$ km for $f = 1$ Hz and $\sigma = 0.1$ S/m. Assuming that the amplitude of this 1-Hz signal is initially A, it will be reduced to nearly $A\exp(-d/1.59)$ after propagating upward to the surface from a depth of d km. For $d = 17.6$ km, the reduced amplitude is $1.56 \times 10^{-5} A$, and clearly the signal is greatly attenuated on reaching the surface. For frequencies near 10 Hz, the signals would have to be extraordinarily strong to be measurable at the surface, and for $f \geq 100$ Hz the δ value would be so great that it is difficult to see how they could be observed at the surface under the assumed conditions.

Because the dipole model produces signal amplitudes that vary in agreement with our observations—that is, they are strongest at 0.01 Hz, weak in the frequency range 1–10 Hz, and cannot be observed above 10 Hz—we now extend this model to estimate the range of the ULF sig-

nals, using the dipole-field data computed by Fraser-Smith and Bubenik (1980). Although these data were intended for field computations involving harmonic dipole sources immersed in the sea, they are presented quite generally and can be used equally well to compute the fields produced at the Earth's surface by dipoles situated beneath the surface (the modeling is subject to the condition that the Earth can be represented by a semi-infinite medium of uniform electrical conductivity). Following Fraser-Smith and Bubenik (1980), we do not consider either a vertical magnetic dipole (VMD) or a vertical electric dipole (VED) as a source, because the magnetic fields generated by a VMD drop off particularly quickly with distance and those generated by a VED tend to be comparatively very small. This consideration leaves either a horizontal electric dipole (HED) or a horizontal magnetic dipole (HMD) as a possible source, of which an HED appears most reasonable in terms of piezomagnetic- or electrokinetic-effect source models for the Loma Prieta magnetic fields.

We first assume that the source is an HED situated close to the hypocenter. The maximum magnetic field of 0.01 Hz measured before the earthquake was close to 60 $nT/\sqrt{Hz}$, or about 5 nT when the bandwidth of the measurement is taken into account. We also assume that Earth has $\sigma=0.1$ S/m, in which case, as discussed above, the dipole will be close to 1 skin depth beneath the surface. Referring to the data of Fraser-Smith and Bubenik (1980) for an HED and an azimuthal angle $\phi=0°$ (that is, along the direction of the axis of the dipole), we find that the magnetic field at the surface directly above an HED buried at 1 skin depth is entirely horizontal and has an amplitude of 1.46×10^{-4} pT for a unit-moment HED. For an azimuthal angle $\phi=90°$, (for example, in a direction perpendicular to the axis of the dipole) an HED generates the same total magnetic field, but it is divided between horizontal and vertical components; we assume that the azimuthal angle is $\phi=0°$. Because the observed maximum magnetic field at Corralitos was 5 nT and Corralitos was nearly directly above the hypocenter of the earthquake, our assumed HED must have had a moment (for example, an electric moment) of about $5,000/1.46\times10^{-4}$, or 3.4×10^7 A·m. A similar computation for an assumed HMD gives a (magnetic) moment of 2.1×10^{11} A·m^2.

To complete the range computation, we need to know the normal background noise of 0.01-Hz magnetic-field fluctuations. We assume that this normal background noise is typically that for August 1989 at Corralitos (fig. 3), which was about 300 to 600 $pT/\sqrt{Hz}$, or 25 to 50 pT for the bandwidth of our measurements at 0.01 Hz. Referring once again to the work of Fraser-Smith and Bubenik (1980), we compute that at 0.01 Hz an HED would generate a 6.7-pT horizontal magnetic-field amplitude on the surface at a horizontal range of 10 skin depths (that is, at a range of 159 km), or an amplitude of 27 pT at a range of 6 skin depths (that is, at a range of 95 km). A similar

computation for an assumed HMD gives a magnetic-field amplitude of 9.5 pT at a range of 10 skin depths and of 42 pT at a range of 6 skin depths. Comparing these dipole-field amplitudes with the estimated normal background-noise range of 25 to 50 pT, we see that the dipole fields become comparable to or greater than the background noise only for ranges of 6 skin depths or less. Taking into account our conservative choice of Earth conductivity and the fact that the largest ULF magnetic fields were too large for our system to measure accurately (and thus that the measured amplitudes are probably smaller than the real amplitudes), we conclude that the 0.01-Hz signals observed before the earthquake might have been measurable out to a distance of about 100 km from the epicenter.

DISCUSSION

We emphasize once again that the ULF data discussed here still require further analysis and that additional measurements need to be made in the time interval immediately preceding other similar earthquakes before any of their anomalous features can be said to be precursors to the Loma Prieta earthquake. However, the location of the Corralitos ULF index generator so close to the epicenter of the earthquake, and the timing of the occurrence of the anomalous features, particularly the increase to an exceptionally high activity starting 3 hours before the earthquake, are encouraging. The absence of similar anomalies in the ULF data obtained during two earlier local earthquakes of $M\sim5$, and the analysis of Loma Prieta aftershock data by Fenoglio and others (1991, 1992), suggest a magnitude threshold below which such anomalies are not generated. In the long run, confirmation of these data will require measurements during further moderate to large earthquakes, and we are pleased to report that, with U.S. Geological Survey (USGS) support, we are now operating two additional ULF-magnetic-field-monitoring systems at Parkfield, Calif., where a moderate earthquake is predicted to occur before 1993 (Bakun and Lindh, 1985); and we have further USGS support for the installation of two more ULF systems on two fault segments in southern California where large earthquakes are anticipated in the future.

The absence of any clearly obvious precursory signals in our ELF/VLF measurements during four local earthquakes, including the Loma Prieta earthquake, is consistent with our view that electromagnetic signals with these higher frequencies cannot escape from the Earth if they are generated any deeper than a few kilometers. The hypocenter of the Loma Prieta earthquake, in particular, was comparatively deep for an earthquake along the northern California section of the San Andreas fault, and it would have been essentially impossible for ELF/VLF signals generated at the depth of the hypocenter to have escaped. Nonetheless, it is still conceivable that some kinds of earthquakes may

generate surface electrical effects or other changes that might launch ELF/VLF signals into the atmosphere. Our failure to observe precursory ELF/VLF noise so close to the epicenters of four moderate to large earthquakes, and the negative result of the Henderson and others (1991) satellite study, show that ELF/VLF noise need not be a strong or an obvious feature of every earthquake.

Perhaps the most important aspect of the results presented here is our identification of the frequency range 0.01–1 Hz as a potential "window" for electromagnetic fields that might be generated by earthquakes at depths in the approximate range 0–30 km. Lower frequency electromagnetic-field fluctuations can also escape without difficulty from sources situated within this depth range (and at greater depths), but the paucity of preearthquake observations of electromagnetic signals with frequencies less than 0.01 Hz suggests that lower frequencies are either not generated or only weakly generated. Further experimental and theoretical studies to investigate the possibility of electromagnetic precursors to earthquakes in this frequency "window" are clearly desirable.

ACKNOWLEDGMENTS

REFERENCES CITED

Bakun, W.H., and Lindh, A.G., 1985, The Parkfield, California, earthquake prediction experiment: Science, v. 229, no. 4714, p. 619–624.

Bernardi, Arman, 1989, Remote measurements of geomagnetic activity; signal processing in the presence of uncertainties in autocovariance estimates: Stanford, Calif., Stanford University, Ph.D. thesis, 120 p.

Bernardi, Arman, Fraser-Smith, A.C., McGill, P.R., and Villard, O.G., Jr., 1991, ULF magnetic field measurements near the epicenter of the M_S 7.1 Loma Prieta earthquake: Physics of the Earth and Planetary Interiors, v. 68, no. 1–2, p. 45–63.

Bernardi, Arman, Fraser-Smith, A.C., and Villard, O.G., Jr., 1989, Measurements of BART magnetic fields with an automatic geomagnetic pulsation index generator: Institute of Electrical and Electronics Engineers Transactions on Electromagnetic Compatibility, v. 31, p. 413–417.

Draganov, A.B., Inan, U.S., and Taranenko, Y.N., 1991, ULF magnetic signatures at the earth surface due to ground water flow: a possible precursor to earthquakes: Geophysical Research Letters, v. 18, no. 6, p. 1127–1130.

Fenoglio, M.A., Fraser-Smith, A.C., and Beroza, G.C., 1991, Search for ultra-low frequency electromagnetic signals during the 1989 Loma Prieta earthquake aftershock sequence [abs.]: Eos (American Geophysical Union Transactions), v. 72, supp., p. 330.

Fenoglio, M.A., Fraser-Smith, A.C., Beroza, G.C., and Johnston, M.J.S., in press, Comparison of ultra-low frequency electromagnetic signals with aftershock activity during the 1989 Loma Prieta earthquake sequence: Seismological Society of America Bulletin.

Fraser-Smith, A.C., Bernardi, Arman, McGill, P.R., Ladd, M.E., Helliwell, R.A., and Villard, Jr., O.G., 1990a, Low-frequency magnetic field measurements near the epicenter of the M_S 7.1 Loma Prieta earthquake: Geophysical Research Letters, v. 17, no. 9, p. 1465–1468.

——1990b, ULF, ELF, and VLF electromagnetic field observations close to the epicenter of the M_S 7.1 Loma Prieta earthquake; possible ULF precursors [abs.]: Eos (American Geophysical Union Transactions), v. 71, no. 8, p. 288.

Fraser-Smith, A.C., and Bubenik, D.M., 1980, Compendium of the ULF/ELF electromagnetic fields generated above a sea of finite depth by submerged harmonic dipoles: Stanford, Calif., Stanford University, Stanford Electronic Laboratories Report SEL–79–025, 114 p.

Fraser-Smith, A.C., and Helliwell, R.A., 1985, The Stanford University ELF/VLF radiometer project; measurement of the global distribution of ELF/VLF electromagnetic noise: Institute of Electrical and Electronics Engineers International Symposium on Electromagnetic Compatibility, 1985, Proceedings, p. 305–311.

Fraser-Smith, A.C., Helliwell, R.A., Fortnam, B.R., McGill, P.R., and Teague, C. C., 1988, A new global survey of ELF/VLF radio noise: Conference on Effects of Electromagnetic Noise and Interference on Performance of Military Radio Communication Systems, Lisbon, 1987, Proceedings, p. 4A–1 to 4A–9.

Fraser-Smith, A.C., McGill, P.R., Bernardi, Arman, Helliwell, R.A., and Ladd, M.E., 1991, Global measurements of low-frequency radio noise, in Environmental and space electromagnetics: Tokyo, Springer-Verlag, p. 191–200.

Gokhberg, M.B., Morgounov, V.A., and Aronov, Y.L., 1981, Radiofrequency radiation during earthquakes: Akademiya Nauk SSSR Doklady, v. 248, p. 32–35.

Gokhberg, M.B., Gufel'd, I.L., and Dobrovol'skiy, I.P., 1982a, Sources of electromagnetic precursors of earthquakes: Akademiya Nauk SSSR Doklady, v. 250, p. 15–17.

Gokhberg, M.B., Morgounov, V.A., Yoshino, Toshio, and Tomizawa, I., 1982b, Experimental measurement of electromagnetic emissions possibly related to earthquakes in Japan: Journal of Geophysical Research, v. 87, no. B9, p. 7824–7828.

Henderson, T.R., Sonwalker, V.S., Helliwell, R.A., Inan, U.S., and Fraser-Smith, A.C., 1991, A search for ELF/VLF emissions induced by earthquakes as observed in the ionosphere by the DE–2 satellite [abs.]: Eos (American Geophysical Union Transactions), v. 72, supp., p. 330.

Johnston, M.J.S., 1989, Review of magnetic and electric field effects near active faults and volcanoes in the U.S.A.: Physics of the Earth and Planetary Interiors, v. 57, no. 1–2, p. 47–63.

Larkina, V.I., Migulin, V.V., Molchanov, O.A., Kharkov, I.P., Inchin, A.S., and Schvetcova, V.B., 1989, Some statistical results on very low frequency radiowave emissions in the upper ionosphere over earthquake zones: Physics of the Earth and Planetary Interiors, v. 57, no. 1–2, p. 100–109.

Larkina, V.I., Nalivayko, A.V., Gershenzon, N.I., Gokhberg, M.B., Liperovskiy, V.A., and Shalimov, S.L., 1983, Observations of VLF emission, related with seismic activity, on the Interkosmos–19 satellite: Geomagnetism and Aeronomy, v. 23, p. 684–687.

Mizutani, Hitoshi, Ishido, Tsuneo, Yokokura, Takanobu, and Ohnishi, Shuhei, 1976, Electrokinetic phenomena associated with earthquakes: Geophysical Research Letters, v. 3, no. 7, p. 365–368.

Oike, Kazuo, and Ogawa, Toshio, 1982, Observations of electromagnetic radiation related with the occurrence of earthquakes: Kyoto, Japan, Kyoto University, Disaster Prevention Research Institute Annual Report, v. 25, no. B–1, p. 89–100.

Parrot, M., and Mogilevsky, M.M., 1989, VLF emissions associated with earthquakes and observed in the ionosphere and the magnetosphere: Physics of the Earth and Planetary Interiors, v. 57, p. 86–99.

Rikitake, Tsuneji, 1975, Earthquake prediction: Amsterdam, Elsevier, 357 p.

Serebryakova, O.N., Bilichenko, S.V., Chmyrev, V.M., Parrot, M., Rauch, J.L., LeFeuvre, F., and Pokhotelov, O. A., 1992, Electromagnetic ELF radiation from earthquake regions as observed by low-altitude satellites: Geophysical Research Letters, v. 19, no. 2, p. 91–94.

Shapiro, V.A., and Abdullabekov, K.N., 1982, Anomalous variations of the geomagnetic field in East Fergana—magnetic precursor of the Alay earthquake with M=7.0 (1978 November 2): Royal Astronomical Society Geophysical Journal, v. 68, no. 1, p. 1–5.

Stacey, F.D., 1964, The seismomagnetic effect: Pure and Applied Geophysics, v. 58, no. 1, p. 5–22.

Tate, Joseph, and Daily, William, 1989, Evidence of electro-seismic phenomena: Physics of the Earth and Planetary Interiors, v. 57, no. 1–2, p. 1–10.

U.S. Geological Survey staff, 1990, The Loma Prieta, California, earthquake; an anticipated event: Science, v. 247, no. 4940, p. 286–293.

Varotsos, P., and Lazaridou, M., 1991, Latest aspects of earthquake prediction in Greece based on seismic electric signals: Tectonophysics, v. 188, no. 3–4, p. 321–347.

Watt, A.D., Mathews, F.S., and Maxwell, E.L., 1963, Some electrical characteristics of the earth's crust: Institute of Electrical and Electronics Engineers Proceedings, v. 51, no. 6, p. 897–910.